

**THE ROLE OF PERTURBATION ON BIOCHEMICAL SYSTEMS: SALT, PH,
AND MICROGRAVITY EFFECTS ON PROTEIN-LIGAND AND SMALL
MOLECULE INTERACTIONS**

A Thesis

Submitted to the Graduate Faculty of the
Louisiana State University and
Agricultural and Mechanical College
in partial fulfillment of the
requirements for the degree of
Master of Science

in

The Department of Biological Sciences

By
Gregory S. Thompson
B.S., Millsaps College, May 2001
May, 2005

PREFACE

This thesis is composed of two relatively independent chapters. The first chapter focuses on work done on type I DNA polymerases from *Escherichia coli*, *Thermus aquaticus*, and *Deinococcus radiodurans*. The second chapter describes the steps taken to prepare a mobile-laboratory to measure reaction rates of molecular interactions on-board NASA's KC-135 microgravity aircraft. While a long range goal of this research is to characterize polymerase function in microgravity, this thesis describes two parallel projects which have not yet merged.

TABLE OF CONTENTS

PREFACE.....	ii
ABSTRACT.....	v
CHAPTER 1. CHARACTERIZATION OF TYPE I DNA POLYMERASES FROM <i>ESCHERICHIA COLI</i> , <i>THERMUS AQUATICUS</i> , AND <i>DEINOCOCCUS RADIODURANS</i>	1
INTRODUCTION.....	1
MATERIALS AND METHODS.....	4
Klenow and Klenoq Purification.....	4
Construction of the Klendein Expression Plasmid.....	4
Klendein Purification Protocol.....	8
DNA Binding.....	10
CD Spectroscopy.....	13
Data Analysis.....	13
RESULTS AND DISCUSSION.....	15
Klenoq and Klenow Show Varying Affinity for DNA in Differing Salts.....	15
Klenoq Structure Dependence of DNA Binding.....	22
Predicted Properties of Klendein Polymerase.....	24
CD Spectroscopy of Klendein Polymerase.....	28
Klendein Has an Invariant T _m vs. pH.....	28
CONCLUSIONS.....	31
REFERENCES.....	33
CHAPTER 2. EFFECTS OF MICROGRAVITY ON PROTEIN-LIGAND AND SMALL MOLECULE INTERACTIONS.....	37
INTRODUCTION.....	37
MATERIALS AND METHODS.....	40
Cart Design and Construction.....	40
DCIP and Ascorbic Acid Reactions.....	46
Data Analysis.....	46
RESULTS AND DISCUSSION.....	47
“In-Lab” Reaction Characterization.....	47
“In-flight” Experiments, pH 6.....	49
“In-flight” Experiments, pH 9.....	54
CONCLUSIONS.....	57
REFERENCES.....	57
APPENDIX 1 OLIGONUCLEOTIDE PRIMERS USED.....	59
APPENDIX 2 SEQUENCE ALIGNMENTS.....	61

APPENDIX 3 13/20MER BINDING IN ACETATE.....	65
APPENDIX 4 KLENTAQ STRUCTURE DEPENDENCE OF BINDING.....	66
APPENDIX 5 PH 6 DCIP AND ASCORBIC ACID REACTIONS MEASURED ON-BOARD KC-135.....	67
APPENDIX 6 PH 9 DCIP AND ASCORBIC ACID REACTIONS MEASURED ON-BOARD KC-135 VS IN-LAB CONTROL.....	68
VITA.....	69

ABSTRACT

DNA binding by the type I DNA polymerases from *Escherichia coli* (Klenow) and *Thermus aquaticus* (Klentaq) has been examined under varying ionic conditions. Klenow and Klentaq both show increased affinity for DNA substrate in the presence of KAcetate over KCl. Ionic linkage relationships were determined for Klenow and Klentaq in KAcetate. Klenow and Klentaq DNA binding show similar ion releases in KAcetate and KCl (~4-5 ions in Klenow, and ~3-4 ions in Klentaq). Interestingly, Klenow and Klentaq exhibit differential ion release in KGlutamate (~4-5 ions in Klentaq and ~2 ions in Klenow).

DNA structure dependence of binding was examined for Klentaq. Klentaq showed a preference for double-stranded and primed-template DNA over single-stranded DNA. Klentaq binds double-stranded and primed-template DNA ~300 times tighter than single-stranded DNA at similar salt concentrations. Klentaq has a dramatically reduced ion release when binding single-stranded DNA (~1 ion) versus double-stranded or primed-template DNA (~3-4 ions).

To help resolve which DNA binding differences might be related to Klentaq's thermal stability, an evolutionarily close, but non-thermophilic, homologue of Klentaq (Klendein from *Deinococcus radiodurans*) has been expressed, purified, and preliminarily examined. Klendein's circular dichroism (CD) spectrum is similar to Klenow and Klentaq. Further, Klendein's stability was probed by monitoring the loss of secondary structure by CD upon heating. Klendein has an invariant T_m (32°C) over the pH range 7.5-9.5.

A long range goal of the study of the regulation of polymerase-DNA binding by solution conditions will include examining the effects of gravity on the interaction. Although no polymerase experiments have yet been performed in microgravity, as a first step toward this goal, this thesis describes initial equipment construction, modification, and calibration for microgravity measurements. To this end, rates of 2,6-dichloroindophenol (DCIP) reduction by varying ascorbic acid was measured under normal lab conditions and under periods of microgravity, onboard NASA's KC-135 zero gravity aircraft. This reaction is generally used to calibrate stopped-flow instruments. Reduction of DCIP at pH 6 was determined to be 850-1000 $M^{-1}sec^{-1}$ under 1g conditions and under microgravity. The reduction of DCIP at pH 9 was determined to be 250-390 $M^{-1}sec^{-1}$ under 1g conditions and under microgravity.

CHAPTER 1

CHARACTERIZATION OF TYPE I DNA POLYMERASES FROM *ESCHERICHIA COLI*, *THERMUS AQUATICUS*, AND *DEINOCOCCUS RADIODURANS*

Introduction

Type I DNA polymerases, also called pol A or pol I, are proteins that catalyze the addition of DNA nucleotides to the 3' hydroxyl of a growing DNA chain, in a primer dependent, template-directed manner. The model protein of this group is the type I DNA polymerase from *Escherichia coli*. It contains 3 structure/function domains common to most pol I's described (Joyce and Steitz, 1995). Figure 1.1 shows the pol I from *Thermus aquaticus* (Eom et al, 1996). Shown in red is the polymerase domain, which catalyzes the addition of nucleotides. Bound to the polymerase domain, and shown in yellow, is DNA. In the polymerizing mode, DNA binds in the deep cleft of the domain, which has been described as a "half-opened" right hand, complete with a "fingers," "thumb," and "palm" sub-domains. The other two domains are the 3'-exonuclease domain (green) which, in Klenow and other pol I's with functional exonuclease domains, catalyzes the removal of nucleotides in a proofreading manner, and the 5'-nuclease domain (shown in blue) which catalyzes the removal of nucleotides in a downstream primer removal function. Together the 3'-exonuclease domain and the polymerase domain form the "large fragment," which when purified from *E. coli*, is referred to as the Klenow fragment (Derbyshire et al, 1993). Further, this large fragment is referred to as Klentaq from *Thermus aquaticus*, and Klendein from *Deinococcus radiodurans*.

Deinococcus radiodurans is a remarkable organism, which is able to repair its DNA from massive DNA damage with remarkable fidelity (Battista, 1997). The

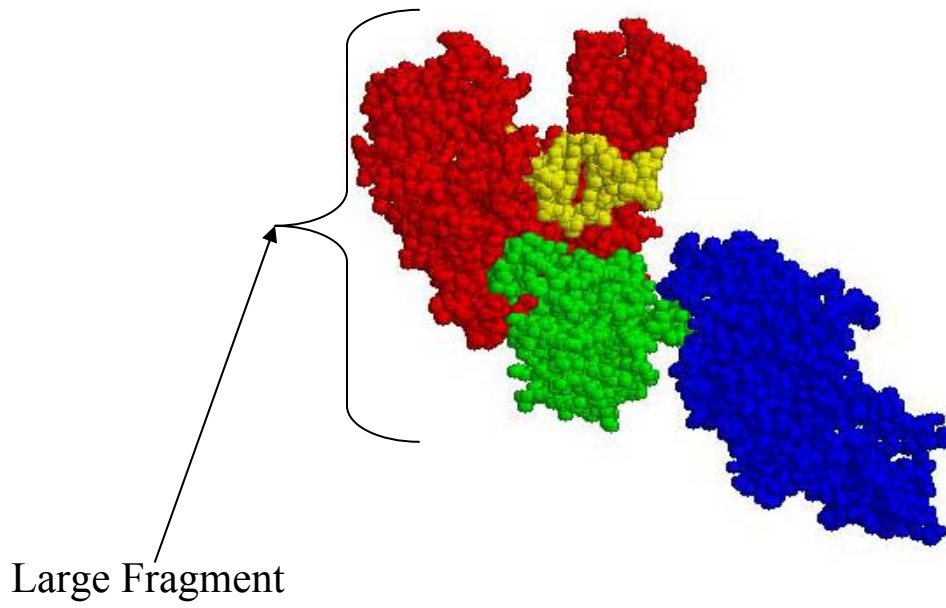


Figure 1.1: Type I DNA polymerase from *Thermus aquaticus*. (PDB accession code: 1TAU)

Deinococcus-Thermus group is believed to be one of the earliest branches of eubacterial evolution. Indeed, this branch is thought to have diverged approximately 2.5 billion years previous to the branch which bore *E. coli* (Battistuzzi et al., 2004). As mentioned, *Deinococcus radiodurans* has the ability to repair its genomic material from catastrophic DNA damage. Damage caused by most DNA damaging agents can be repaired; including double stranded DNA breaks, DNA nicks, nucleotide crosslinking, and individual base modifications (Minton, 1994. Makarova et al, 2001). There are a number of proteins which are absolutely essential for *D. radiodurans*' DNA repair capabilities, including pol I (Gutman et al., 1994).

Studies by Minton, et al. (1994) discounted a unique role of *D. radiodurans*' pol I in accelerated DNA repair. This result was determined by supplementing polymerase knockout mutant strains of *D. radiodurans* (pol⁻) with full-length pol I and Klenow fragment from *E. coli*. *E. coli* pol I was able to restore near wild-type resistance to UV radiation, γ -radiation, and Mitomycin C exposure. Klenow was able to restore wild-type resistance to γ -radiation and Mitomycin C exposure, but failed to restore full resistance to UV radiation, indicating a possible role of the 5'-exonuclease domain in *D. radiodurans* UV damage repair response. However, the paper fails to address a number of key issues, the most pressing of which is the cellular concentration of pol I found in the supplemented pol⁻ mutants. The authors describe a system where the pol I gene is inserted as 50 tandem copies of sequence per chromosome, resulting in "substantial expression" of the pol I genes. The authors fail to demonstrate a comparable supplemented polymerase concentration, relative to the wild-type. Perhaps 50X *E. coli*

pol I can substitute for 1X *D. radiodurans* pol I. A crucial question is whether 1X *E. coli* pol I can substitute for 1X *D. radiodurans* pol I. This paper fails to address this issue.

Multiple techniques have been employed to investigate the physical differences between type I DNA polymerases in vitro. These investigations routinely find that homologous proteins from different organisms do not necessarily behave similarly (Perler et al., 1996). Instead, individual organisms' DNA polymerases seem to have evolved as a result of various environmental factors, including heat, salinity, and pH. It is the goal of this chapter to: 1.) Report results collected that illustrate some of these functional differences between Klenow and Klentaq. 2.) Describe the steps taken to clone, express, and purify Klendein DNA polymerase from *Deinococcus radiodurans*. It is the long range goal of this project to determine the unique physical properties of Klendein DNA polymerase, so that we may understand its functional relationships to Klentaq and Klenow, and that we may more clearly understand its role in the DNA repair response in *Deinococcus radiodurans*.

Materials and Methods

Klenow and Klentaq Purification: Klenow and Klentaq were purified as described previously (Derbyshire et al., 1993, Datta and LiCata, 2003).

Construction of the Klendein Expression Plasmid: Expression plasmids (pGT002 and pGT003) carrying the full length pol I gene or the large fragment Klendein gene, were constructed from PCR amplified *Deinococcus radiodurans* R1 strain genomic material provided as a gift from Dr. John Battista (Louisiana State University). The full-length pol I gene was amplified and inserted into a pET15b expression plasmid using NcoI and BamHI restriction sites, engineered using mutagenic primers at the N- and C-

termini of the gene (all primers used in cloning are shown in Appendix 1) (White et al., 1999).

The large fragment gene was sub-cloned from the full length clone, using PCR to introduce an NcoI cut site at the start of the large fragment portion of the protein. The Klendein gene was inserted into a pET15b expression plasmid, from Novagen (Figure 1.2).

Sequence alignments of Klenow and Klentaq with their respective full length protein sequences were used to determine the appropriate site for construction of the Klendein fragment. Sequence alignments were performed using ClustalW sequence alignment software, provided with the BioEdit Software suite (Hall, 1999). The full sequence alignments are shown in Appendix 2, and the alignment of the three full-length proteins and the large-fragment proteins around the cut-site can be seen in Figure 1.3. This alignment was used to determine where in the full-length sequence for *D. radiodurans*' pol I, a Klenow analogous fragment could be constructed. Klenow and Klentaq align to within eight residues of each other, so it was clear that Klendein should begin in that vicinity. Klendein's specific start site was chosen to eliminate a rare CCC proline codon in the N-terminal region, a codon that could have served as a "bottle-neck" during protein production.

The plasmid pGT003 was fully sequenced and checked against published sequences (Makarova et al., 2001). Two deviations from published sequences were discovered. Nucleotide position 412 was discovered to be G, while the published sequence at this position is A. Additionally, nucleotide 757 was discovered to be C, while the published sequence at this position is A. Residues were returned to the published sequence

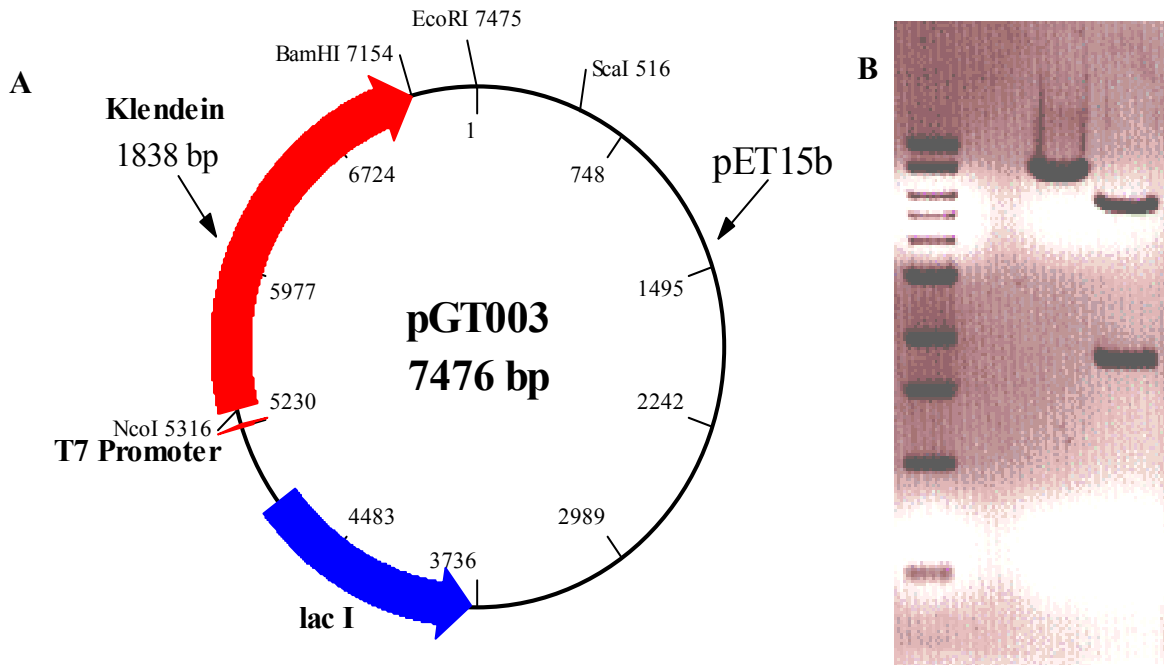


Figure 1.2: Panel A: Plasmid map of pGT003 plasmid, showing the Klendein gene inserted into a pET15b expression vector. **Panel B:** (L-R) 1kb MW standard, pGT003 linearized with NcoI, and pGT003 digested with NcoI and BamHI.

```

E. coli pol I      K Y E F K R W T A D V E A G K W L Q A K G A K P A A K P Q E T S V A D E A P E V
T. aquaticus pol I  - - - - - E F G S L L H - - - - -
D. radiodurans pol I - - - - - L E L H S L R P M I L G L N G P E Q D G H A P D D L L E R E H A
Klenow           - - - - -
Klentaq         - - - - -
Klendeim        - - - - -

E. coli pol I      T A T V I S Y D N Y V T I L D E E T L K A W I A K L E K A P V F A F D T E T D S
T. aquaticus pol I  - - - - - E F G L L E S P K A L E E A P W P - P P E G A - F V G F V L S R K -
D. radiodurans pol I Q T P E E D E A A A L P A F S A P E L A E W Q T P A E G A - V W G Y V L S R E -
Klenow           - - - V I S Y D N Y V T I L D E E T L K A W I A K L E K A P V F A F D T E T D S
Klentaq         - - - - - M S P K A L E E A P W P - P P E G A - F V G F V L S R K -
Klendeim        - - - - - M A F S A P E L A E W Q T P A E G A - V W G Y V L S R E -

E. coli pol I      L D N I S A N L V G L S F A I E P G V A A Y I P V A H D Y L D A P D Q I S R E R
T. aquaticus pol I  - E P M W A D L L A L A A A A R G - G R V H R A P E P - - - - -
D. radiodurans pol I - D D L T A A L L A A A T F E D - G V A R P A P V S E P D E W A Q A E A P E N L
Klenow           L D N I S A N L V G L S F A I E P G V A A Y I P V A H D Y L D A P D Q I S R E R
Klentaq         - E P M W A D L L A L A A A A R G - G R V H R A P E P - - - - -
Klendeim        - D D L T A A L L A A A T F E D - G V A R P A P V S E P D E W A Q A E A P E N L

```

Figure 1.3: Multi-protein alignment excerpt showing N-terminal residues of Klendeim, Klenow, and Klentaq aligned with their respective full-length pol I's.

using site-directed mutagenesis (Wang and Malcolm, 1999). The corrected plasmids were named pGT005 for full length pol I, and pGT006 for Klendein. Interestingly, various reports have shown that some sequences from the R1 strain of *D. radiodurans* vary from the published genomic sequence (Eggington et al., 2004). It remains unclear whether these mutations are genetic variations present in different strains of *D. radiodurans*, or if they were generated randomly during the cloning. It should be noted, however, that in all cases the most accurate commercially available polymerase, *PfuUltra* DNA polymerase from Stratagene was used during both the PCR and the site-directed mutagenesis in order to maintain the fidelity of the gene (Lundberg et al., 1991).

Klendein Purification Protocol: Klendein was expressed by introduction of 1mM isopropyl-B-D-thiogalactopyranoside (IPTG), to a one liter culture of BL-21 (DE3) Rosetta cells (Novy et al, 2001) carrying the Klendein expression plasmid pGT006, once the culture reached a growth of 0.5 ODU. Induction was allowed to proceed for 12-16 hours. Cells were harvested by centrifugation, and resuspended in Lysis Buffer (10mM Tris-HCl, 5mM MgCl₂, 250mM KCl, 250mM Glucose, pH 7.9), phenylmethanesulfonyl fluoride (PMSF) was added to 1mM. Lysozyme was added to 1 mg/ml and cells were sonicated, until lysed. (Figure 1.4)

Neutral pH poly(ethyleneimine) (PEI) was added to a final concentration of 0.25-0.30% to precipitate Klendein and nucleic acid. Klendein was resuspended from the insoluble portion in KTA (10mM Tris, 5 mM MgCl₂, 22 mM NH₄SO₄, pH 7.0) + 250mM KCl, with a dounce homogenizer.

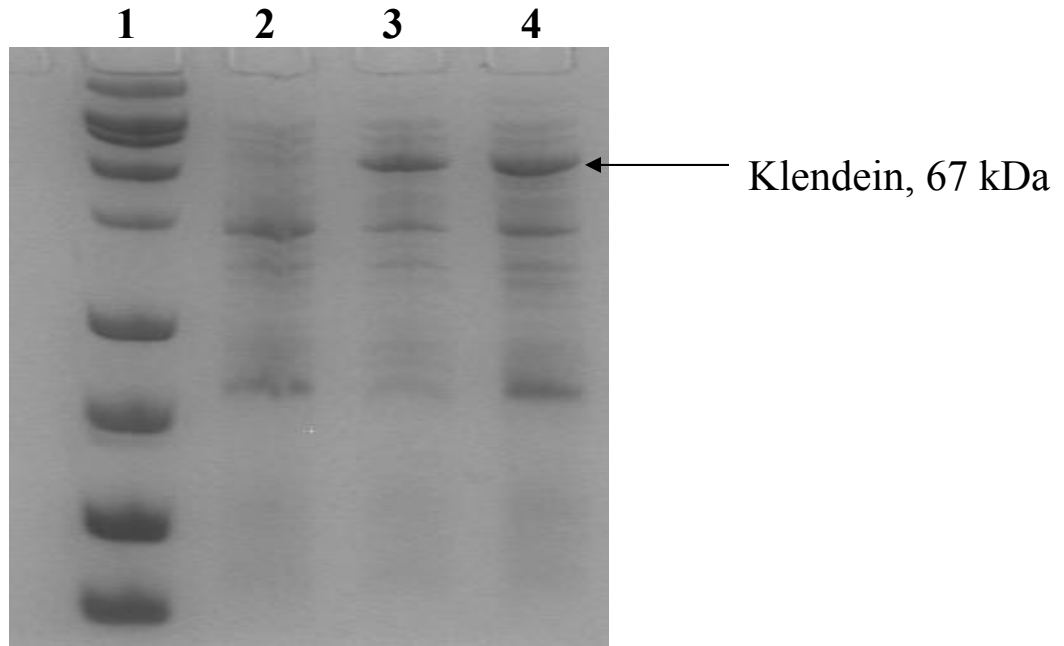


Figure 1.4: Expression of Klendein polymerase. Klendein was expressed in BL21(DE3)-Rosetta cells for 0 (lane 2), 4 (lane 3), and 16 hours (lane 4), and run next to a MW standard (lane 1).

Resuspended protein was run over a Bio-Rex 70 cation exchange column (Scott et al., 1978), pre-equilibrated with KTA at pH 7.0. The protein was allowed to bind the column and then eluted with a 0-750mM KCl in KTA. (Figure 1.5)

Appropriate fractions were collected and run on a gel. The Bio-Rex 70 eluate was found to contain a number of contaminating proteins. Protein solution was further purified over an immobilized Heparin column pre-equilibrated with KTA at pH 7.0, and eluted with a 22-270mM Ammonium Sulfate gradient. The protein was determined, via SDS-gel electrophoresis, to be pure. (Figure 1.6) To this point, however, the protein yield has been prohibitively low to allow exhaustive characterization. Typically, a 1L preparation yields 0.5 mg of purified protein, an amount sufficient for initial spectroscopic characterization but not for calorimetric or kinetic analysis which require significantly more protein.

DNA Binding: To determine the DNA binding affinity of Klendein polymerase, Rhodamine-X (ROX) labeled DNA was titrated with increasing protein concentration, in an assay previously used to characterize Klenow and Klentaq DNA binding (Datta and LiCata, 2003). All protein was extensively dialyzed into 10mM Tris, and appropriate salt as indicated, at pH 7.9. Binding was followed by monitoring the fluorescence anisotropy signal change as protein-DNA complex is formed. Anisotropy was measured using an ISS Koala spectrofluorometer with automatic polarizers, by exciting the probe at 583 nm and monitoring the fluorescence with a 600 nm cut-off filter. All protein and DNA was extensively dialyzed into 10 mM Tris, and appropriate salt as indicated, at pH 7.9.

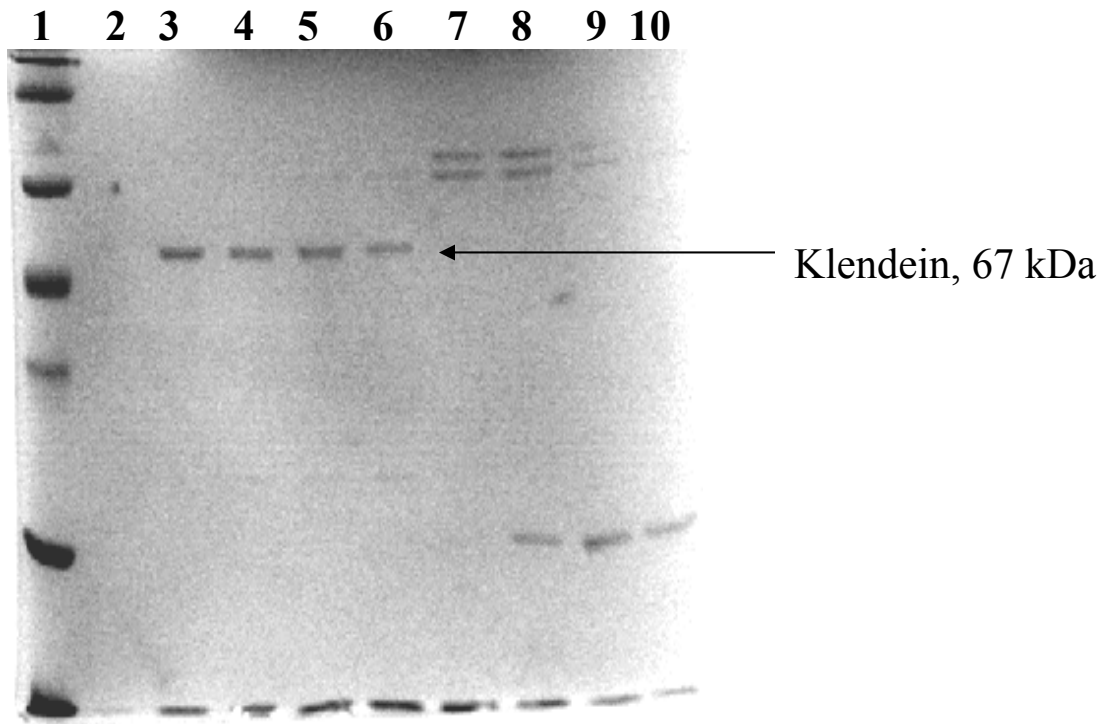


Figure 1.5: Representative Bio-Rex 70 elution profile. Lanes (L – R) were: Lane 1, SDS-Broad Range MW Standard; Lane 2, Column flow through; Lanes 3-10, Protein fractions collected as column was eluted with 0-750 mM KCl salt gradient.

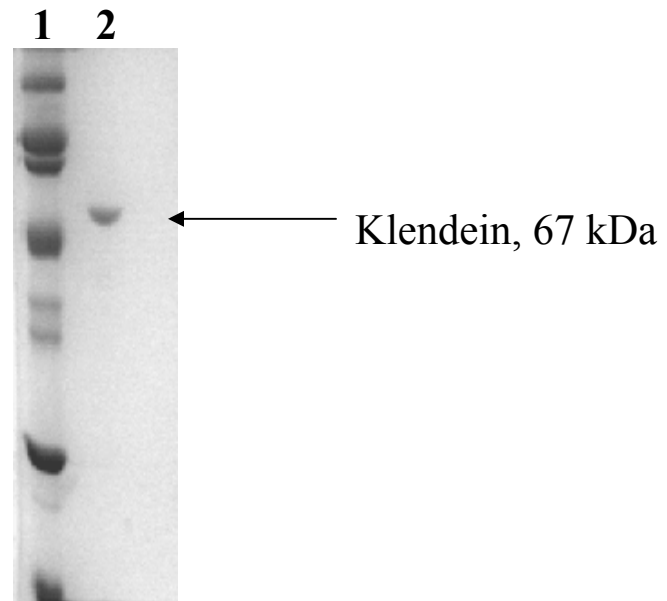


Figure 1.6: Heparin column elution. Left lane shows a MW standard, while lane 2 contains purified protein. Klendein's calculated Mw is 67 kDa, which runs a bit above the 66 kDa MW standard.

All DNA constructs used in the binding assays were purchased from Integrated DNA Technologies, the construct's sequences were as follows:

63/70mer: 5'-TACGCAGCGTACATGCTCGTGACTGGGATAACCGTGCCGTTTG-
3'-ATGCGTCGCATGTACGAGCACTGACCCTATTGGCACGGCAAAC-
CCGACTTTCGCAGCCGTCCA-3'
GGCTGAAAGCGTCGGCAGGTTCCCAAA-5'

13/20mer: 5'-TCGCAGCCGTTCCA-3'
3'-AGCGTCGGCAGGTTCCCAAA-5'

63mer: 5'-TACGCAGCGTACATGCTCGTGACTGGGATAACCGTGCCGTTTG
CCGACTTTCGCAGCCGTCCA-3'

CD Spectroscopy: CD measurements were recorded using an AVIV Model 202 CD spectrophotometer, at temperatures as noted, controlled by an automatic temperature cyclor. For thermal denaturation plots, CD signal was monitored between 219-222nm, and the temperature steps increased 3°C until the temperature reached 25°C, the temperature was then stepped in 1°C increments, until 50°C. Full spectrum wavelength scans (200-240nm) were performed at 5°C.

Data Analysis: DNA equilibrium binding titration curves were fit to the following equation to determine the equilibrium binding constant (K_d).

$$\Delta A = \{ \Delta A_t (E_t / K_d) / (1 + E_t / K_d) \}$$

(Equation 1.1)

Where A is the measured anisotropy, A_t is the total anisotropy change, and E_t is the total enzyme concentration.

Equilibrium binding constants were determined in varying salt concentrations. The relationship between the binding constant (K_d) and the salt concentration is given by Equation 1.2, and is commonly called a linkage relationship (Wyman, 1964. Lohman et al., 1978).

$$\left\{ \frac{\partial \ln(1/K_d)}{\partial \ln[salt]} \right\} = \Delta n_{ions} = \Delta n_{cations} + \Delta n_{anions}$$

(Equation 1.2)

Thus, a plot of $\ln(1/K_d)$ vs. $\ln[salt]$ will yield a straight line, whose slope is equal to the net number (Δn) of ions released or taken up upon ligand binding. These plots are generally termed “linkage plots.”

Thermal denaturation plots were fit to a modified van't Hoff equation (Equation 1.3), where the slope of the native (m_n) and denatured state (m_d) baselines are fit simultaneously with the transition region to determine the T_m and the ΔH (Ramsay and Eftink, 1994). T_m 's reported here represent the average of four measurements determined at 218nm, 219nm, 220nm, and 221nm wavelengths.

$$\Delta \varepsilon = (m_n T + b_n) + (m_d T + b_d) \left(\frac{K}{1 + K} \right)$$

where

$$K = \exp \left[-\Delta H \left(1 - \frac{T}{T_m} \right) / RT \right]$$

(Equation 1.3)

Results and Discussion

The initial portion of the results section will describe several aspects of the physical characterization of type I DNA polymerases Klenow and Klentaq, with emphasis on new data collected as part of this thesis. The latter half of the section will describe the results collected thus far on Klendein DNA polymerase.

Klenow and Klentaq Show Varying Affinity for DNA in Differing Salts:

Equilibrium DNA binding titrations were performed for both Klenow and Klentaq binding 13/20mer DNA in varying concentrations of KAcetate, in order to determine the effects of various salts on the protein-nucleic acid equilibrium. Figure 1.7 shows representative binding titrations for Klenow in increasing concentrations of KAcetate, in the absence of added Mg^{2+} . As expected, the K_d for the protein-nucleic acid interaction increased with higher salt, as ions act “competitively” to destabilize the protein-DNA complex. This relationship is common for protein-nucleic acid equilibria, and indicates a net positive number of ions released upon complex formation (Wyman, 1964. Lohman et al., 1978).

Appendix 3 shows the K_d 's for Klenow and Klentaq binding 13/20mer in various concentrations of KAcetate measured with and without Mg^{2+} . Linkage plots were established from this data to determine the net linked ion release upon 13/20mer binding.

Klenow polymerase was titrated over 300-500mM KAcetate, with and without Mg^{2+} . Klenow's linkage in KAcetate was determined to be 4.9 ± 0.5 ions released upon DNA binding in the presence of Mg^{2+} , and 4.4 ± 0.4 ions released in the absence of Mg^{2+} . (Figure 1.8)

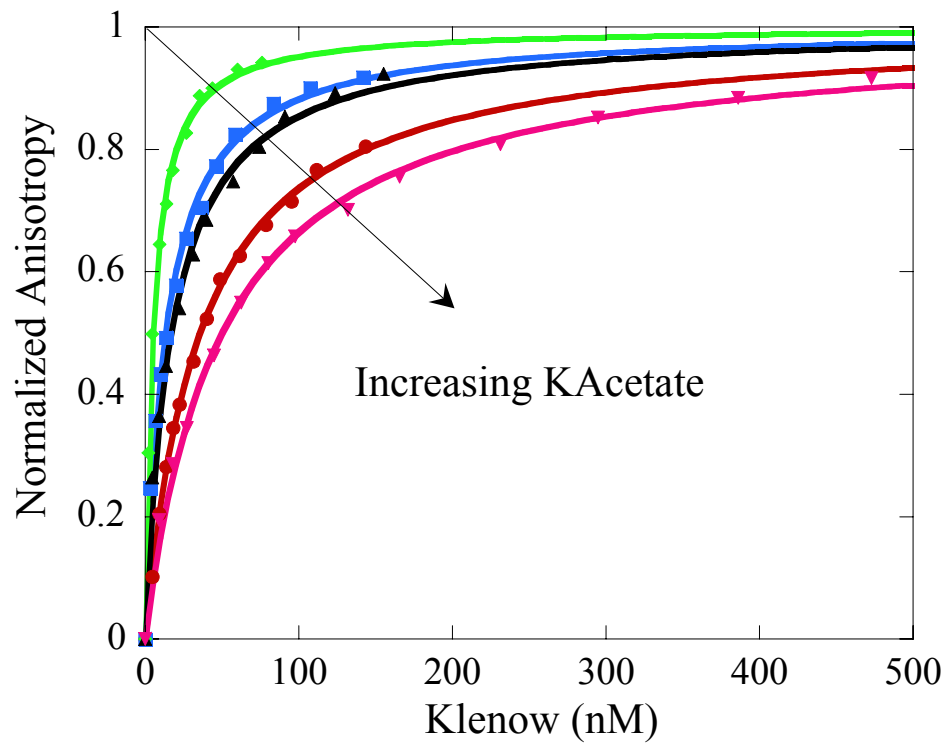


Figure 1.7: Representative DNA binding curves for Klenow binding 13/20mer DNA, in increasing concentrations of KAcetate. 300mM KAcetate (green diamonds), 350mM (blue squares), 400mM (black triangles), 450mM (red dots), 500mM (pink inverted triangles).

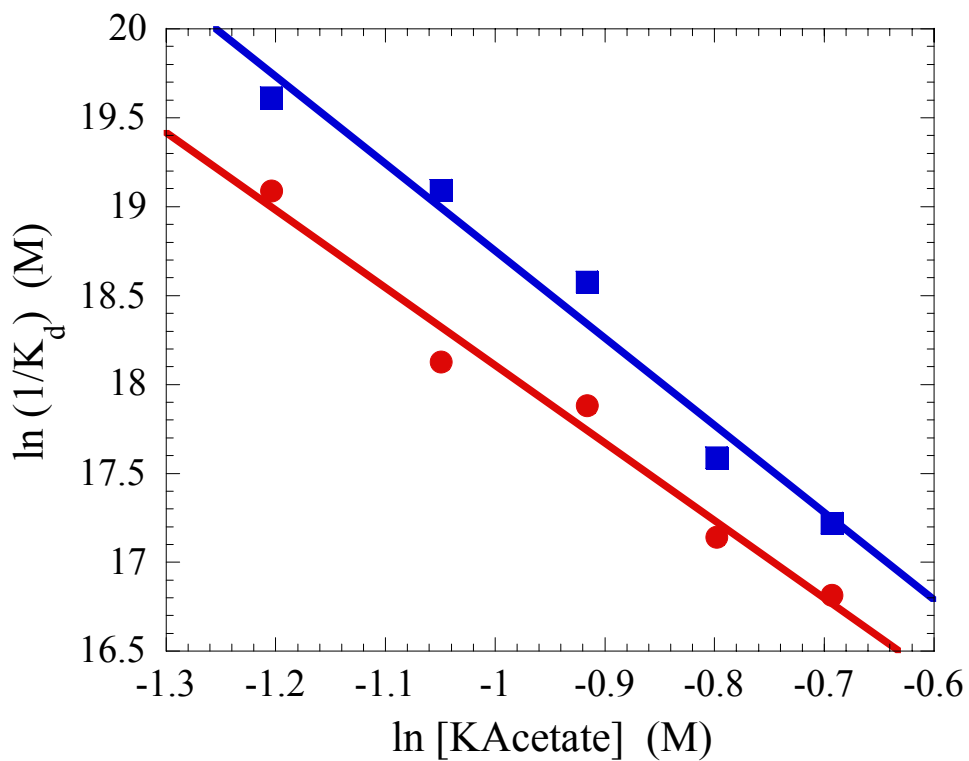


Figure 1.8: Linkage plot of Klenow binding 13/20mer DNA in varying concentrations of KAcetate, with (blue squares) and without (red dots) 5mM Mg^{2+} .

Additionally, Klentaq was titrated in varying concentrations of KAcetate with and without Mg^{2+} . (Figure 1.9) Klentaq's linkage was found to be 3.4 ± 0.25 ions released upon DNA binding in the presence and 3.8 ± 0.2 ions released in the absence of Mg^{2+} . Klentaq, like Klenow, has a small linkage or affinity change in the presence or absence of Mg^{2+} .

Figures 1.10 and 1.11 compare data from this thesis with previous salt dependence studies of Klenow and Klentaq. It has been shown that many DNA binding protein's affinities and linkages are significantly altered in varying anions (Barkley et al., 1981. Lohman and Mascotti, 1992. Ha et al., 1992. Overman and Lohman, 1994). Figure 1.10 shows Klentaq binding 13/20mer DNA in varying concentrations of KCl. (Datta and LiCata, 2003), KAcetate (this thesis), and 2 racemers of KGlutamate. (Daniel Deredge, unpublished results) In all salts, Klentaq releases approximately 3-4 net ions.

Klenow, however, shows varying linkage upon DNA binding in these same salts. Klenow releases approximately 4-5 ions in the presence of KCl (Datta and LiCata, 2003) and KAcetate (this thesis), but drops to ~ 2 ions in the presence of either form of KGlutamate (Daniel Deredge, unpublished results). (Figure 1.11)

This differential linkage in KGlutamate has been commonly called the "glutamate effect." (Ha et al., 1992) The glutamate effect has been observed in numerous DNA binding systems, however, this is the first observation of homologous proteins from different organism where one, and not the other, exhibits this effect. There are several mechanisms that could explain the Klenow/Klentaq results. 1.) Klenow may contain a specific Cl-/Acetate binding site, not present in Klentaq. Thus, more anions are released from Klenow when ligand binds. *E. coli* Single Stranded Binding Protein (SSB) has been

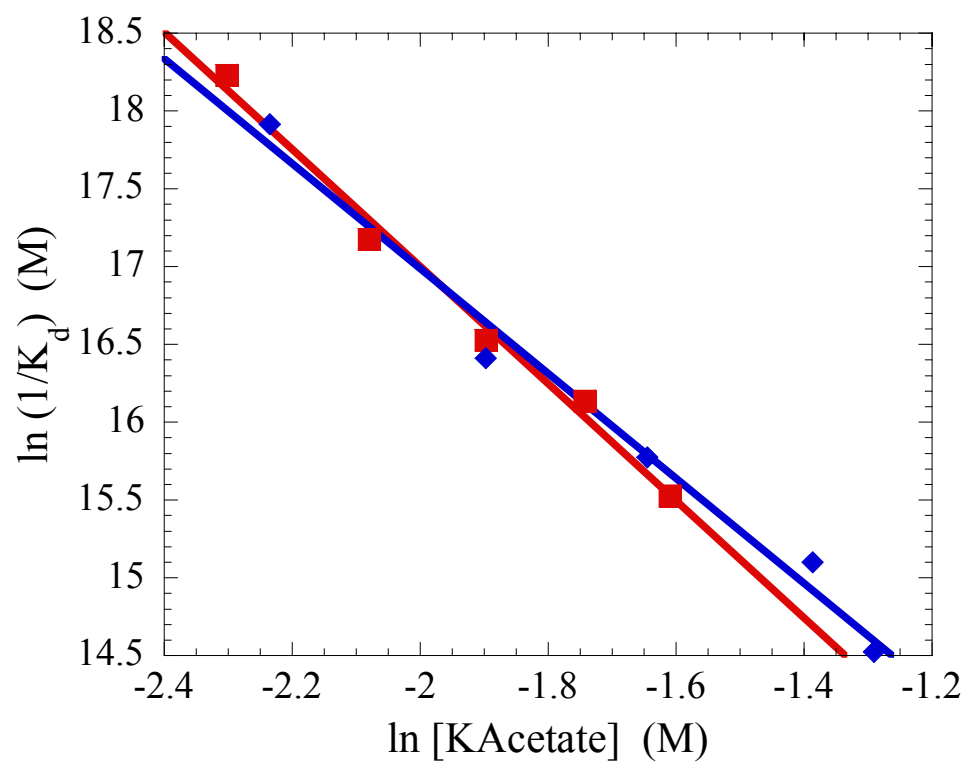


Figure 1.9: Linkage plot of Klentaq binding 13/20mer DNA in varying concentrations of KAcetate, with (blue diamonds) and without (red squares) 5mM Mg^{2+} .

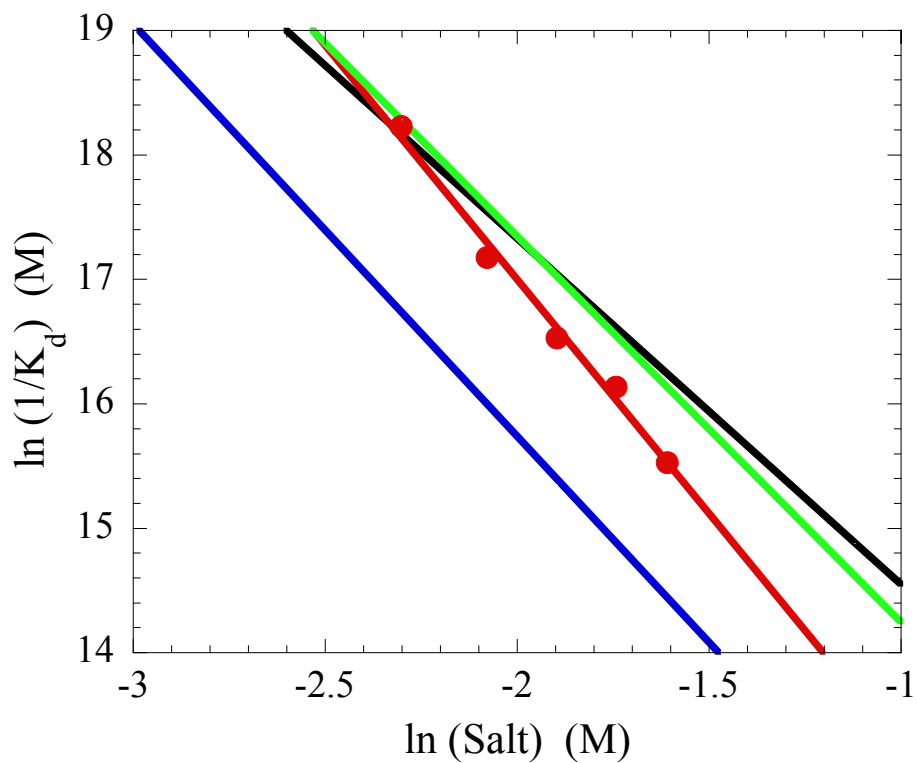


Figure 1.10: Linkage plot of KlenTaq binding 13/20mer DNA in various salts. Slope of the line is proportional to the number of net ions released or taken up upon ligand binding. Linkage was established in KCl (blue line), Acetate (red dots), D-Glutamate (green line), and L-Glutamate (black line).

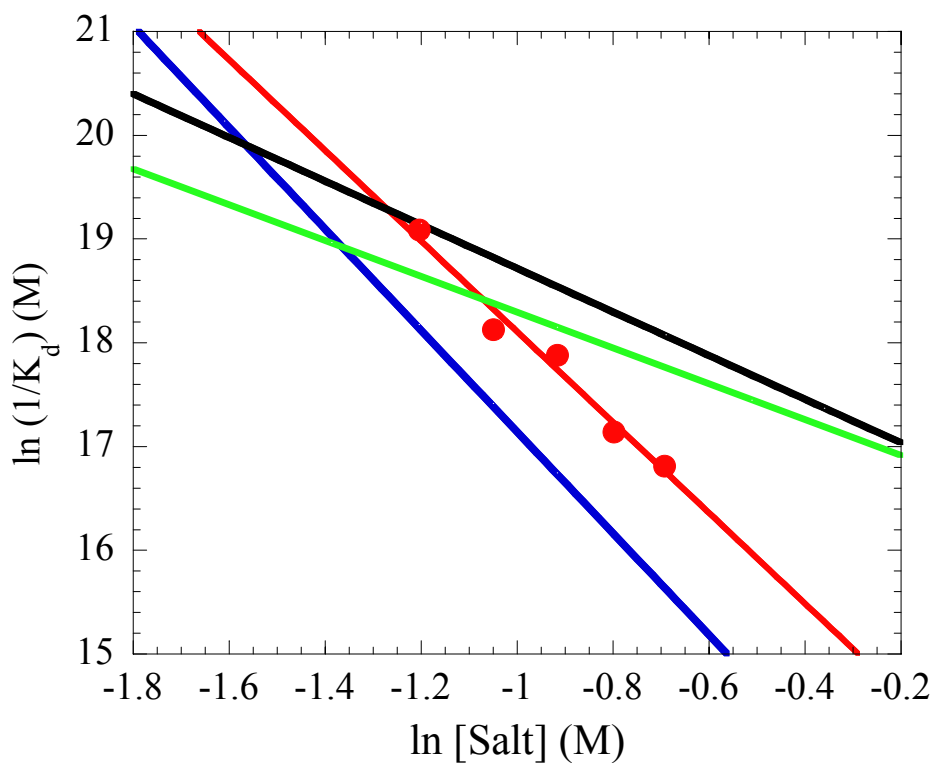


Figure 1.11: Linkage plot of Klenow binding 13/20mer DNA in various salts. Slope of the line is proportional to the number of net ions released or taken up upon ligand binding. Linkage was established in KCl (blue line), Acetate (red dots), D-Glutamate (green line), and L-Glutamate (black line).

shown to have specific Cl⁻ binding sites, which exclude other ions. This specificity leads to the same types of differential linkages seen in Klenow (Overman and Lohman, 1994).

2.) Glutamate could be specifically taken up as a part of a Klenow-DNA complex, reducing the net linkage effect, if the glutamate participates in the formation of salt bridges to the phosphate backbone. 3.) Glutamate may act as an allosteric effector of Klenow, which when taken up by the protein causes Klenow to adopt a high affinity binding conformation, which leads to a tighter binding constant at all salt concentrations measured, as well as a reduced linkage in this salt. This last option deserves further consideration. While this option seems less likely, given the invariant effect of both D- and L- isomers of KGlutamate, we cannot rule out that a small, yet specific, portion of the glutamate molecule is interacting with a potential allosteric site. It would be impossible for the protein to differentiate D- and L- isomers; if for example, the allosteric site only binds the carboxylic acid side chain.

Klentaq Structure Dependence of DNA Binding: Invariably, all DNA polymerases encounter a number of potential substrate molecules *in vivo*. In order to determine the extent to which DNA polymerases screen potential ligands, I measured the affinity of Klentaq for different DNA structures at varying KCl concentrations. Figure 1.12 shows the linkage plots when Klentaq binds single-stranded 63mer DNA, double-stranded 63/63mer DNA, and primed-template 63/70mer DNA. Interestingly, Klentaq shows almost no preference for its assumed “natural” ligand, primed-template DNA, over double-stranded DNA at this temperature. At elevated temperatures, binding to primed-template DNA is favored (Andy Wowor, unpublished results). However, it is impossible

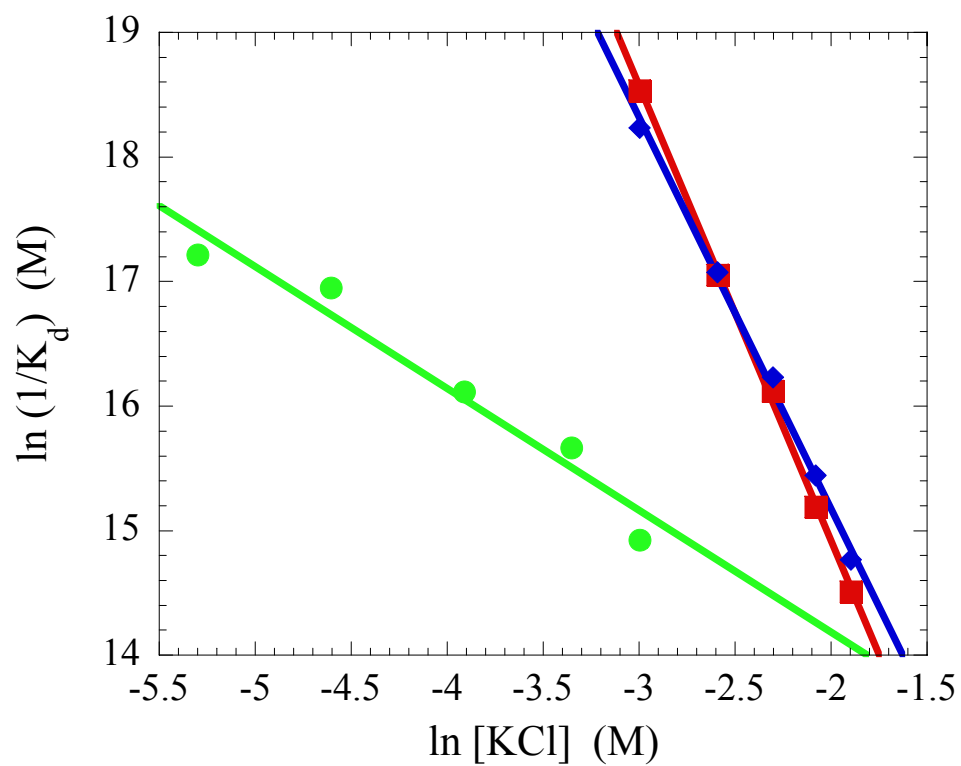


Figure 1.12: Linkage plots generated when KlenTaq binds 63mer (green dots), 63/70mer (red squares), and 63/63mer DNA (blue diamonds). All experiments were performed at 25°C.

to determine from this data set whether KlenTaq has a high affinity for double-stranded DNA or if it has a preference for DNA double-stranded breaks, known as an “end-binder” (King et al., 1994. King et al., 1996).

KlenTaq binds single stranded DNA with a significantly reduced affinity relative to the other substrates and at a lower salt concentration range. In addition, the linkage is reduced from 3-4 ions released, down to 1. It is generally believed that the greatest contribution to a linkage in protein nucleic acid interactions comes from cation release from the negatively-charged phosphodiester backbone of the nucleic acid (Ha et al., 1992). The dramatically reduced linkage when KlenTaq binds single-stranded DNA may argue for significant non-specific nucleotide base interactions with the protein’s surface driving single-stranded DNA binding, rather than a predominantly surface-backbone interaction.

Predicted Properties of Klendein Polymerase: Klendein’s amino acid sequence was subjected to multiple protein alignments, structure prediction programs, and other property prediction resources. Figure 1.13 shows a predicted protein structure using the SWISS-MODEL program available from the SWISS-PROT protein database (Schwede et al., 2003). This model was generated using sequence and structural homology to other DNA polymerases for which crystal structures have been determined. This model relied heavily upon the crystal structures of both Taq DNA polymerase and Klenow polymerase. It is not surprising then, that the predicted structure shares many features common to other type I DNA polymerases structures solved to date. The model shows the characteristic half-opened right hand structure where DNA binds in the deep cleft between the finger and thumb regions. As well, the predicted structure is predominantly



Figure 1.13: 3D-Model generated using SWISS-MODEL software available from SWISS-PROT protein database. (<http://swissmodel.expasy.org/>)

α -helical, a characteristic of both Klentaq and Klenow. Klendein's sequence was submitted to the PredictProtein Server (<http://cubic.bioc.columbia.edu/predictprotein/>), a protein secondary structure prediction server. Klendein was predicted to have 58.3% α -helical content, 6.4% extended structure (the structure most likely to form β -sheets), and 35.3% loop (or disordered) structures (Rost and Sander, 1993). For comparison, PredictProtein Server predicted that Klenow has 49.8% α -helical content while Klentaq contains 56.3%.

It has been well established that Klentaq polymerase does not have a functioning 3'-exonuclease domain, while Klenow's is fully functional (Beese and Steitz, 1991). Further, the residues important for 3' domain functionality have been established in Klenow (Beese and Steitz, 1991. Derbyshire et al., 1991). In order to try and predict whether or not Klendein contains a functional 3'-exonuclease domain, I used sequence alignments of Klenow, Klentaq, and Klendein (Figure 1.14). The residues directly implicated in 3' domain functionality in Klenow are Asp 355, Glu 357, Asp 424, Asp 501, Phe 473, Tyr 497 (Derbyshire, et al. 1991). The acidic residues are believed to be involved in chelating the Mg^{2+} ions necessary for the catalytic mechanism of the domain, while the aromatic residues are believed to orient a water molecule involved in the nucleophilic attack of the phosphate backbone (Derbyshire et al., 1991).

The alignment (Figure 1.14) shows that none of these 6 critical residues in Klenow are conserved in Klendein or Klentaq. It has been shown that even a single mutation to one of the carboxylic acid residues is sufficient to destroy catalytic activity of the exonuclease domain in Klenow (Derbyshire et al., 1991). Indeed, the common exo^- mutant of Klenow is a D424A mutant, the natural change exhibited by both Klendein and

```

                                * *
Klenow  VISYDNYVTILDEETLKAWIAKLEKAPVFVAFDTETDSDLNISANLVGLSFAIEPGVAAYI
Klentaq -----MSPKALEEAPWP-PPEGA-FVGFVLSRK--EPMWADLLALAAARG-GRVHRA
Klendein -----MAFSAPELAEWQTPAEGA-VWGYVLSRE--DDLTAALLAAATFED-GVARPA

                                *
Klenow  PVAHDYLDAPDQISRERALELLKP-----LLEEDEKALKVGNLKYDRGILAN-----
Klentaq PEP-----YKALRDLKEARGLL-----
Klendein PVSEPDEWAQAEAPENLFGELLPSDKPLTKKEQKALEKAQKDAEKARAKLREQFPATVDE

                                *
Klenow  -----YGIELRGIAFDTMLESYILNSVAGRHDMSLAERWLKHKTIITFEEIAGKGNQLT
Klentaq -----AKDLSVLALREGLGLPPGDDPMLLAYLLDPSNTTPEGVARR-----
Klendein AEFVQRTVTAAAALAAHLSVRGTVVEPGDDPLLYAYLLDPANTNMPVVAKR-----

                                * *
Klenow  FNQIALEEAGRYAAEDADVTLQLHLKMWPDLQKHKGPLNVFENIEMPLVPVLSRIERNGV
Klentaq ---YGG-EWTEEAGERAAALSERLFANLWGRLEGEERLLWLYREVERPLSAVLAHMEATGV
Klendein ---YLDREWPADAPTRAAITGHLRELPLLLDDARR--KMYDEMEKPLSGVLGRMEVRGV

Klenow  KIDPKVLHNNSEELTLRLAELEKKAHEIAGEEFNLSSTKQLQTILFEKQGIKPKKTPG-
Klentaq RLDVAYLRALSLEVAEEIARLEAEVFRLAGHPFNLSRDQLERVLFDELGLPAIGKTEKT
Klendein QVDSDFLQTLSIQAGVRLADLESQIHEYAGEEFHIRSPKQLETVLYDKLELASSKKTKLT

Klenow  GAPSTSEEVLEELALDYPLPKVILEYRGLAKLKSTYTDKLPLMINPKTGRVHTSYHQAVT
Klentaq GKRSTSAAVLEALREAHPIVEKILQYRELTKLKSTYIDPLPDLIHPRTGRLHTRFNQTAT
Klendein GORSTAVSALEPLRDAHPIIPLVLEFRELDKLRGTYLDPINLVNPHTGRLHTTFAQTAV

Klenow  ATGRLSSDPNLQNIPVRNEEGRRIRQAFIAPEDYVIVSADYSQIELRIMAHLSRDKGLL
Klentaq ATGRLSSDPNLQNIPVRTPLGQRIRRAFIAEEGWLLVALDYSQIELRVLAHLSGDENLI
Klendein ATGRLSSLNPNLQNIPIRSELGREIRKGFIAEDGFTLIAADYSQIELRLLAHIADDPLMQ

Klenow  TAFEAGKDIHRATAAEVFLPLETVTSEQRSSAKAINFGLIYGMSAFGLARQLNIPRKEA
Klentaq RVFQEGRDIHTETASWMFGVPREAVDPLMRRAAKTINFGVLYGMSAHRLSQELAIPYEEA
Klendein QAFVEGADIHRRTAAQVLGLDEATVDANQRRAAKTVNFGVLYGMSAHRLSNDLGIPYAEA

Klenow  QKYMDLYFERYPGVLEYMERTRAQAKEQGYVETLDGRRLYLPDIKSSNGARRAAAERAAI
Klentaq QAFIERYFQSFPKVRAWIEKTLEEGRRRGYVETLFGRRRYVPDLEARVKSVREAAERMAF
Klendein ATFIEIYFATYPGIRRYINHTLDFGRTHGYVETLYGRRRYVPGLSSRNRVQREAEERLAY

Klenow  NAPMQGTAADIIKRAMIAVDAWLQAEQPRVRMIMQVHDELVFEVHKDDVDAVAKQIHQLM
Klentaq NMPVQGTAADLMKLAMVKLFPRLEEMG--ARMLLQVHDELVLEAPKERAEAVARLAKEVM
Klendein NMPIQGTAADIMKLAMVQLDPQLDAIG--ARMLLQVHDELLIEAPLDKAEQVAALTTKVM

Klenow  ENCTRLDVPLLVEVGSGENWDQAH-
Klentaq EGVYPLAVPLEVEVGIGEDWLSAKE
Klendein ENVVQLKVPLAVEVGTGPNWFDTK-

```

Figure 1.14: Alignment of Klenow, Klentaq, and Klendein. Asterisks (*) indicate residues demonstrated to be important for 3'-exonuclease functionality. In order, D355, E357, D424, F473, Y497, and D501.

Klentaq. The alignment predicts that Klendein will have a non-functional 3'-exonuclease domain. This finding could be extremely interesting, if this prediction is valid, given the essential role of pol I in *D. radiodurans*' DNA repair response. After catastrophic DNA damaging events, little or no mutation is seen in *D. radiodurans*' restored genome, implying that the DNA polymerase involved in repair functions with very high fidelity. Together, these results imply other DNA polymerases may play important roles in *D. radiodurans*' DNA damage repair. Interestingly, a pol X from *Deinococcus radiodurans* has been identified and has been shown to be important in the organism's response to double stranded DNA damage as caused by γ -radiation. (Lecoite et al., 2004)

CD Spectroscopy of Klendein Polymerase: In order to confirm that purified Klendein was properly folded, the protein was subjected to CD spectrophotometry. Figure 1.15 shows wavelength scans of purified Klenow, Klentaq, and Klendein performed from 200 nm to 240 nm to determine the major secondary structural elements present.

The CD wavelength scan of Klendein is characteristic of a protein which is predominantly α -helical, as its spectra exhibits the two peaks, at $\sim 208\text{nm}$ and $\sim 221\text{nm}$ (Greenfield and Fasman, 1969. Pelton and McLean, 2000). Indeed, Klendein's spectra is similar to those of Klentaq and Klenow measured under the same conditions (Chin-Chi Liu, unpublished results).

Klendein has an Invariant T_m vs pH: Klendein denaturation was monitored by loss of secondary structure in the CD spectrophotometer, upon heating from 10°C to 50°C (Figure 1.16). The denaturation curves measured at 218-221nm, were fit to Equation 1.3. The average T_m of the protein was determined to be 32.1°C . The optimal growth

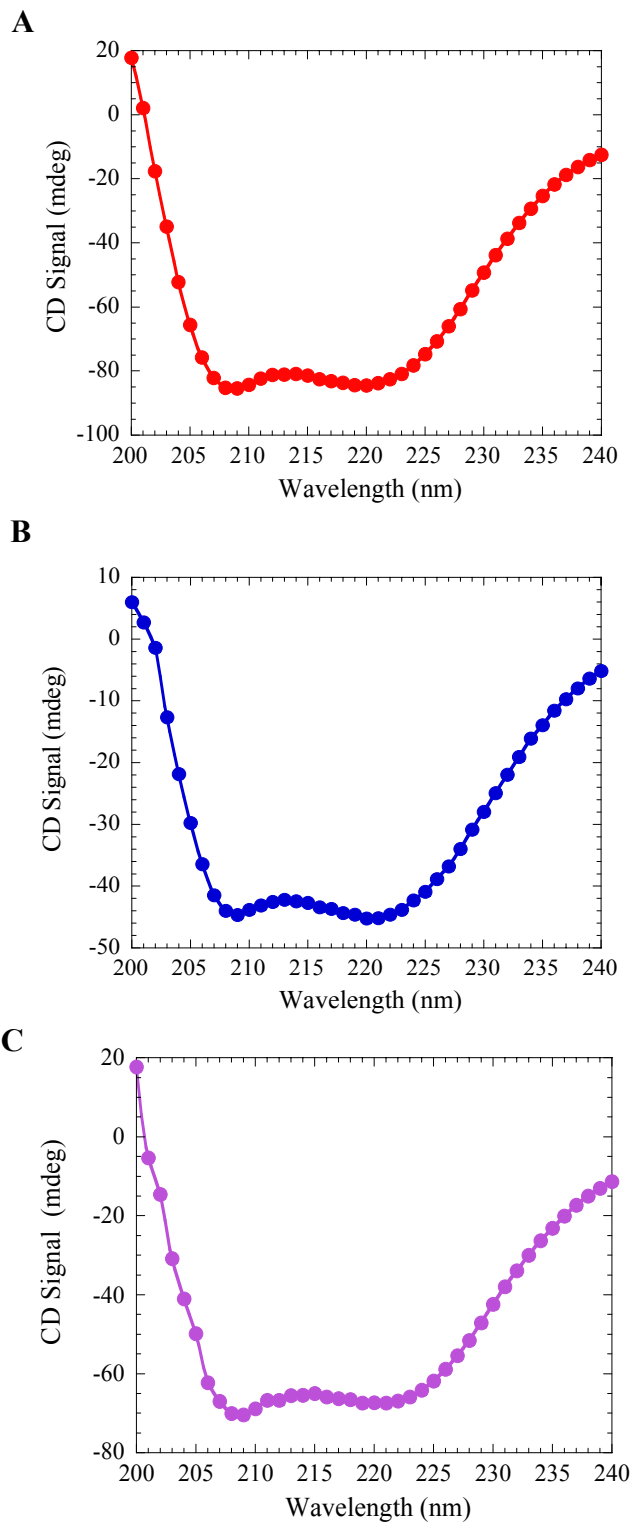


Figure 1.15: CD wavelength scans of Klenow (**Panel A**-red dots), Klentaq (**Panel B**-blue dots), and Klendein (**Panel C**-purple dots) at 5°C.

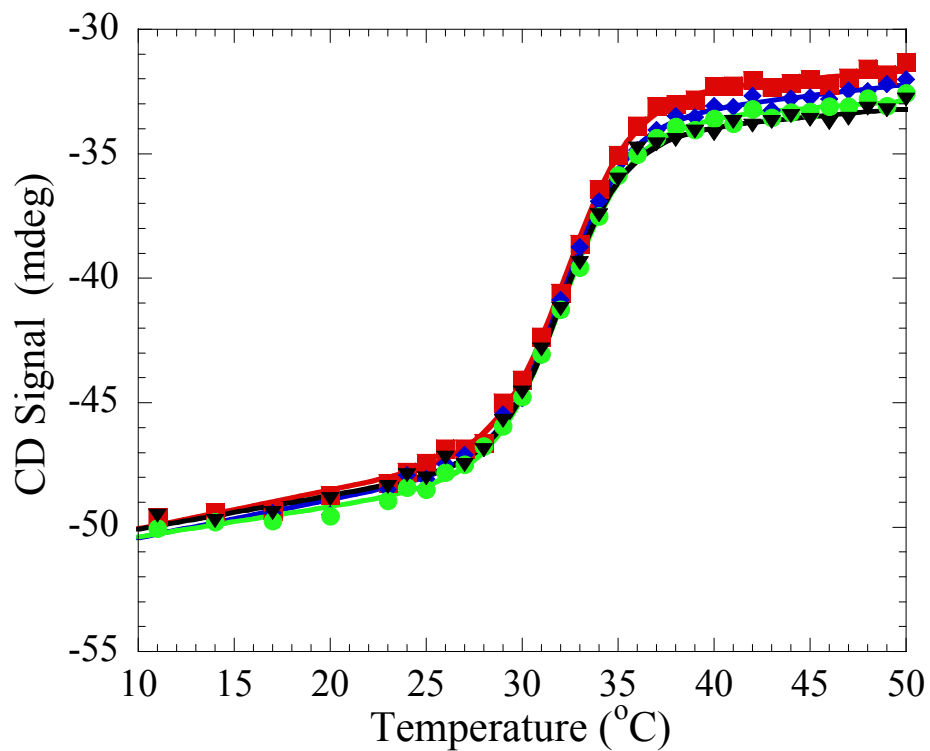


Figure 1.16: Thermal denaturation plots monitored at 218 nm (red squares), 219 nm (blue diamonds), 220 nm (green dots), and 221 nm (black triangles) in pH 9.5 10mM PO₄ buffer. Data was fit to Equation 1.3, to determine the T_m of the protein.

temperature of *D. radiodurans* is 30°C. The protein is likely further stabilized by other compounds in vivo.

Klenow and Klentaq had been previously subjected to thermal denaturation. Both Klenow and Klentaq showed a very strong pH dependence on the T_m (Karantzeni et al., 2003). In order to investigate the extent to which pH could stabilize Klendein, the protein was melted over a 2 pH unit range, from 7.5-9.5. While Klenow and Klentaq each demonstrated a significant T_m changes in varying pH, (Figure 1.17) Klendein's T_m is invariant in different pH buffers.

A decreasing T_m vs. increasing pH in the basic pH range could be caused by stabilizing electrostatic interactions on the protein surface, which become weaker upon increased deprotonation of basic residues. These results suggest Klendein does not have any of these types of titratable residues with pKa's within the pH range measured, while Klenow and Klentaq do.

Conclusions

Results presented in this thesis illustrate some of the physical differences between three homologous proteins; Klenow, Klentaq, and Klendein. The results presented illustrate the importance of in vitro characterization of homologous proteins from diverse organisms.

Klenow and Klentaq exhibit differential ion binding capabilities in their DNA binding domains. Examining the linkage and affinity changes of protein-ligand interactions is a powerful tool when exploring the protein's potential function in vivo. It is well-known that organisms regulate their intracellular environments carefully. These studies demonstrate a practical reason for such care.

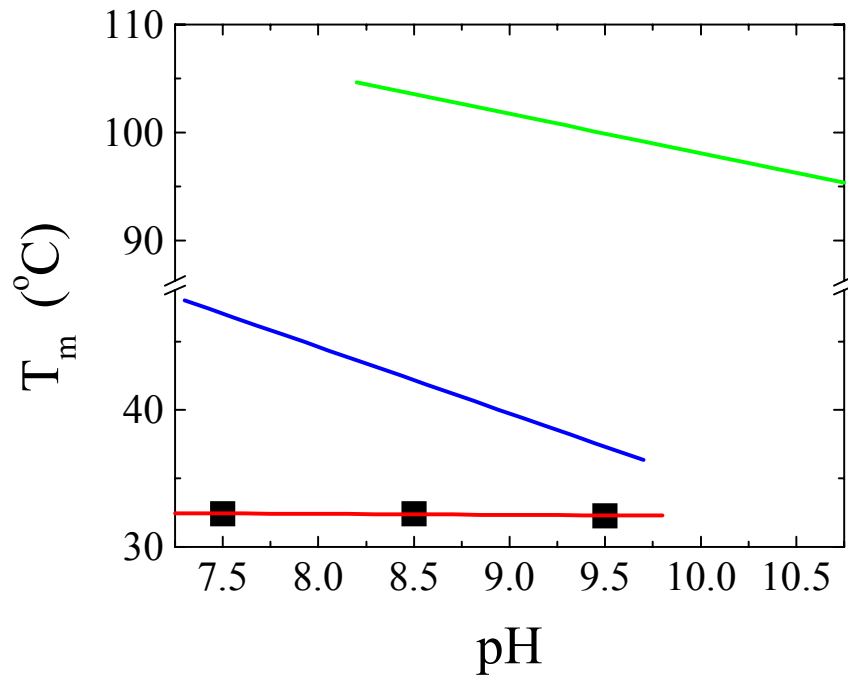


Figure 1.17: A T_m vs. pH profile for Klendein polymerase (red line, black squares), vs. Klenow (blue line) and Klentaq (green line).

Klentaq exhibits strong structural preference for double-stranded DNA over single-stranded DNA. Conversely, similar studies with Klenow demonstrate a preference for single-stranded substrate over double-stranded DNA (Andy Wowor, unpublished results). Understanding the functional significance of this preference is an ongoing goal of this project. Similar studies with Klendein should be performed, and the range of potential ligands should be expanded to match the types of constructs Klendein may encounter during DNA damage repair, including damaged bases and branched DNA constructs common in recombinatorial DNA repair. Complete characterization of Klendein's binding preferences will give us a better functional understanding of *D. radiodurans*' DNA repair response in vivo.

Klendein has an invariant T_m over the pH range measured. This finding suggests a reduced number of stabilizing salt bridges on the surface of Klendein. Many theories exist to describe the way thermophilic proteins are able to survive exposure to very high temperatures. A common theory is the presence of an additional number of stabilizing salt bridges on the surface of the thermophilic protein relative to the mesophile. Close phylogenetic relatives (like Klentaq and Klendein) with dramatically differing T_m vs. pH profiles, could be used to determine the presence of salt bridges important for thermophilicity. Indeed, this possibility is currently being employed in our lab.

References

- Barkley, M. D., Lewis, P. A., and Sullivan, G. E. (1981) Ion Effects on the Lac Repressor—Operator Equilibrium. *Biochemistry*. **20 (13)**: 3842-3851.
- Battistuzzi, F. U., Feijao, A., and Hedges, S. B. (2004) A genomic timescale of prokaryote evolution: insights into the origin of Methanogenesis, Phototrophy, and the Colonization of Land. *BMC Evolutionary Biology*. **4**: 44-58

- Battista, J. R. (1997) Against All Odds: The Survival Strategies of *Deinococcus radiodurans*. *Annu. Rev. Microbiol.* **51**: 203-224.
- Beese, L. S., and Steitz, T. A. (1991) Structural Basis for the 3'-5' Exonuclease Activity of *Escherichia coli* DNA Polymerase I: A Two Metal Ion Mechanism. *EMBO.* **10 (1)**: 25-33.
- Datta, K., and LiCata, V. J. (2003) Salt Dependence of DNA binding by *Thermus Aquaticus* and *Escherichia coli* DNA Polymerases. *J. Biol. Chem.* **278 (8)**: 5694-5701.
- Derbyshire, V., Astatke, M., and Joyce, C. M. (1993) Re-engineering the Polymerase Domain of Klenow Fragment and Evaluation of Overproduction and Purification Strategies. *N. A. R.* **21 (23)**: 5439-5448.
- Derbyshire, V., Grindley, N. D., and Joyce, C. M. (1991) The 3'-5' Exonuclease of DNA Polymerase I of *Escherichia coli*: Contribution of Each Amino Acid at the Active Site of the Reaction. *EMBO.* **10 (1)**: 17-24.
- Derbyshire, V., Pinsonneault, J. K., and Joyce, C. M. (1995) Structure-Function Analysis of 3'-5'-Exonuclease of DNA Polymerases. *Methods.* **262**: 363-385.
- Eggington, J. M., Haruta, N., Wood, E.A., and Cox, M. M. (2004) The single-stranded DNA-binding protein of *Deinococcus radiodurans*. *BMC Microbiol.* **4 (1)**: 2.
- Eom, S.H., Wang, J., and Steitz, T. A.. (1996) Structure of Taq polymerase with DNA at the polymerase active site. *Nature.* **382**: 278-281.
- Greenfield, N. and Fasman, G.D. (1969) Computed circular dichroism spectra for the evaluation of protein conformation. *Biochemistry.* **8(10)**: 4108-4116
- Gutman, P. D., Fuchs, P., and Minton, K. W. (1994) Restoration of the DNA damage resistance of *Deinococcus radiodurans* mutants by *Escherichia coli* DNA polymerase I and Klenow fragment. *Mutat. Res.* **314 (1)**: 87-97.
- Ha, J. H., Capp, M. W., Hohenwarter, M. D., Baskerville, M., and Record, M. T. Jr. (1992) Thermodynamic Stoichiometries of Participation of Water Cations and Anions in Specific and Non-Specific Binding of Lac Repressor to DNA. Possible Thermodynamic Origins of the "Glutamate Effect" on Protein-DNA Interactions. *J. Mol. Biol.* **228 (1)**: 252-264.
- Hall, T. A. (1999) BioEdit: A User-Friendly Biological Sequence Alignment Editor and Analysis Program for Windows 95/98/NT. *Nucl. Acids Symp. Ser.* **(41)**: 95-98.
- Heyduk, T., Ma, Y., Tang, M., and Ebright, R. H. (1996) Fluorescence Anisotropy: Rapid, Quantitative Assay for Protein-DNA and Protein-Protein Interactions. *Methods.* **274**: 492-503.

Joyce, C. M., and Steitz, T. A. (1995) Polymerase Structures and Function: Variations on a Theme? *J. of Bact.* **177 (22)**: 6321-6329.

Karantzeni, I., Ruiz, C., Liu, C., and LiCata, V. J. (2003) Comparative Thermal Denaturations of *Thermus aquaticus* and *Escherichia coli* Type I DNA Polymerases. *Biochem. J.* **374**: 785-792.

King, J. S., Fairley, C. F., and Morgan, W. F. (1994) Bridging the Gap: Joining of Nonhomologous Ends by DNA Polymerases. *J. Biol. Chem.* **269 (18)**: 13061-13064.

King, J. S., Fairley, C. F., and Morgan, W. F. (1996) DNA End Joining by the Klenow Fragment of DNA Polymerase I. *J. Biol. Chem.* **271 (34)**: 20450-20457.

Lundberg, K. S., Shoemaker, D. D., Adams, M. W., Short, J. M., Sorge, J. A., and Mathur, E. J. (1991) High-Fidelity Amplification Using a Thermostable DNA Polymerase Isolated from *Pyrococcus furiosus*. *Gene*. **108 (1)**: 1-6

Lecoite, F., Shevelev, I. V., Bailone, A., Sommer, S., and Hubscher, U. (2004) Involvement of an X-Family DNA Polymerase in Double-Stranded Break Repair in the Radioresistant Organism *Deinococcus radiodurans*. *Mol. Microbiol.* **53 (6)**: 1721-1730.

Lohman, T. M., de Haseth, P. L., and Record, M. T. (1978) Analysis of Ion Concentration Effects on the Kinetics of Protein-Nucleic Acid Interactions: Application of lac repressor-operator interactions. *Biophys. Chem.* **(8)**: 281-294.

Lohman, T. M., and Mascotti, D. P. (1992) Thermodynamics of Ligand-DNA Interactions. *Methods*. **(212)**: 400-424.

Makarova, K. S., Aravind, L., Wolf, Y. I., Tatusov, R. L., Minton, K. W., Koonin, E. V., and Daly, M. J. (2001) Genome of the Extremely Radiation-Resistant Bacterium *Deinococcus radiodurans* Viewed from the Perspective of Comparative Genomics. *Microbiol. Mol. Biol. Rev.* **65 (1)**: 44-79.

Minton, K. W. (1994) DNA Repair in the Extremely Radioresistant Bacterium *Deinococcus radiodurans*. *Mol. Microbiol.* **13 (1)**: 9-15.

Novy, R., Drott, D., Yaeger, K., and Meirendorf, R. (2001) Overcoming the Codon Bias of *E. coli* for Enhanced Protein Expression. *Innovations*. **(2)**: 1-3.

Overman, L. B., Bujalowski, W., and Lohman, T. M. (1988) Equilibrium Binding of *Escherichia coli* Single-Stranded Nucleic Acids in the (SSB)₆₅ Binding Mode. Cation and Anion Effects and Polynucleotide Specificity. *Biochemistry*. **27 (1)**: 456-471.

Overman, L. B., and Lohman, T. M. (1994) Linkage of pH, Anion and Cation Effects in Protein-Nucleic Acid Equilibria. *Escherichia coli* SSB Protein-Single Stranded Nucleic Acid Interactions. *J. Mol. Biol.* **236 (1)**: 165-178.

Pelton, J. T. and McLean, L. R. (2000) Spectroscopic Methods for Analysis of Protein Secondary Structure. *Anal Biochem.* **277(2)**:167-76

Perler, F. B., Kumar, S., Kong, H. (1996) Thermostable DNA Polymerases. *Adv Protein Chem.* **(48)**: 377-435.

Ramsay, G. D., and Eftink, M. R. (1994) Analysis of Multidimensional Spectroscopic Data to Monitor the Unfolding of Proteins. *Methods.* **240**: 615-645

Rost, B., Sander, C. (1993) Prediction of Protein Secondary Structure at Better than 70% Accuracy. *J. Mol. Biol.* **232(2)**: 584-99.

Saecker, R. M., and Record, T. M. Jr. (2002) Protein Surface Salt Bridges and Paths for DNA Wrapping. *Curr. Opin. Struct. Biol.* **12 (3)**: 311-9.

Schwede, T., Kopp, J., Guex, N., and Peitsch, M. C. (2003) SWISS-MODEL: an Automated Protein Homology-Modeling Server. *Nucleic Acids Res.* **31 (13)**: 3381-3385.

Scott, J. F. and Kornberg, A. (1978) Purification of the Rrep Protein of *Escherichia coli*. An ATPase Which Separates Duplex DNA Strands in Advance of Replication. *J. Biol. Chem.* **253 (9)**: 3292-7.

Wang, W. and Malcolm, B., A. (1999) Two-Stage PCR Protocol Allowing Introduction of Multiple Mutations, Deletions, and Insertions Using Quik-Change Site-Directed Mutagenesis. *Biotechniques.* **26 (4)**:680-2

White, O., Eisen, J. A., Heidelberg, J. F., Hickey, E. K., Peterson, J. D., Dodson, R. J., Haft, D. H., Gwinn, M. L., Nelson, W. C., Richardson, D. L., Moffat, K. S., Qin H., Jiang L., Pamphile, W., Crosby, M., Shen, M., Vamathevan, J. J., Lam, P., McDonald, L., Utterback, T., Zalewski, C., Makarova, K. S., Aravind, L., Daly, M. J., and Fraser, C. M. (1999). Genome Sequence of the Radioresistant Bacterium *Deinococcus radiodurans* R1. *Science.* **286(5444)**:1571-7.

Wyman, J. (1964) Linked functions and reciprocal effects in hemoglobin: A second look. *Adv. Prot. Chem.* **19**: 223-286.

CHAPTER 2

EFFECTS OF MICROGRAVITY ON PROTEIN-LIGAND AND SMALL MOLECULE INTERACTIONS

Introduction

Experiments performed onboard multiple space flights and in simulated microgravity have shown that cells grown under microgravity exhibit severe functional deficiencies. The origin of these cellular problems is unknown; however, some reports have begun to address this problem. Most reports commonly describe functional differences, including depressed cell growth rates, modified signaling pathways, and modified gene expression (Walther et al., 1998. Nickerson et al., 2004). In addition, studies by Papaseit et al (2000), found that microtubule morphology was significantly perturbed under microgravity. A recent review, by Graebe et al, (2004) details the large number of physiological changes that humans undergo when exposed to spaceflight, including cardiovascular problems due to fluid redistribution in the body, bone demineralization and decalcification, altered immunological response, decreased red blood cell count, as well as altered hormone levels. However, very little is known about how the mechanisms of biochemical processes are affected once exposed to weightlessness. Two reports have investigated protein-ligand interactions in microgravity, with differing conclusions. One report (Maccarrone et al, 1998) determined that lipoxygenase's affinity for substrate (K_m) increased 4-fold in the presence of microgravity, without an increase in maximal rate of catalysis (V_{max}). While the enzyme-substrate complex formed more readily, there was no increase in the rate of enzymatic catalysis. These results support the hypothesis that the catalytic rate of

diffusion limited reactions might be most likely to be affected by microgravity, as the slow step in these types of reactions is the protein-ligand association, not the catalytic event. However, a separate report found no remarkable difference between any measurable quantities (K_m , V_{max} , etc.) between 1g controls and microgravity for isocitrate lyase function, from *Pinus pinea* (Ranaldi et al, 2003).

The aim of this chapter is to describe reactions we have measured onboard NASA's KC-135 microgravity laboratory. Over the course of 2 parabolic microgravity flights, we measured the concentration dependence of ascorbic acid on the microscopic pseudo-first order rate constant (k_1) for the reduction of 2,6-dichloroindophenol (DCIP), using a modified stopped-flow fluorometer. The reaction is one which has been used for many years as a "standard" to assure proper functionality of stopped-flow instruments (Tonomura et al., 1978). This reaction was chosen for a number of reasons. 1.) The reagents are relatively inexpensive, which allowed for exhaustive characterization in the laboratory. 2.) The reaction mechanism is well defined. It consists of a complete oxidation of the hydroxyl groups attached to the pyrene ring of ascorbate, with a subsequent reduction of DCIP, as shown in Figure 2.1. 3.) The reaction can be manipulated easily into pseudo-first order reaction conditions. Indeed, the reaction conditions used throughout this thesis are 200-1200 fold excess of ascorbic acid to DCIP. 4.) The reaction is easily monitored. The reaction shows a dramatic loss of blue color on a millisecond timescale, which can be readily monitored with our fluorometer in a modified "absorbance" mode. 5.) The reaction is very pH sensitive. At low pH the reaction occurs very rapidly, while at higher pH the reaction occurs much more slowly.

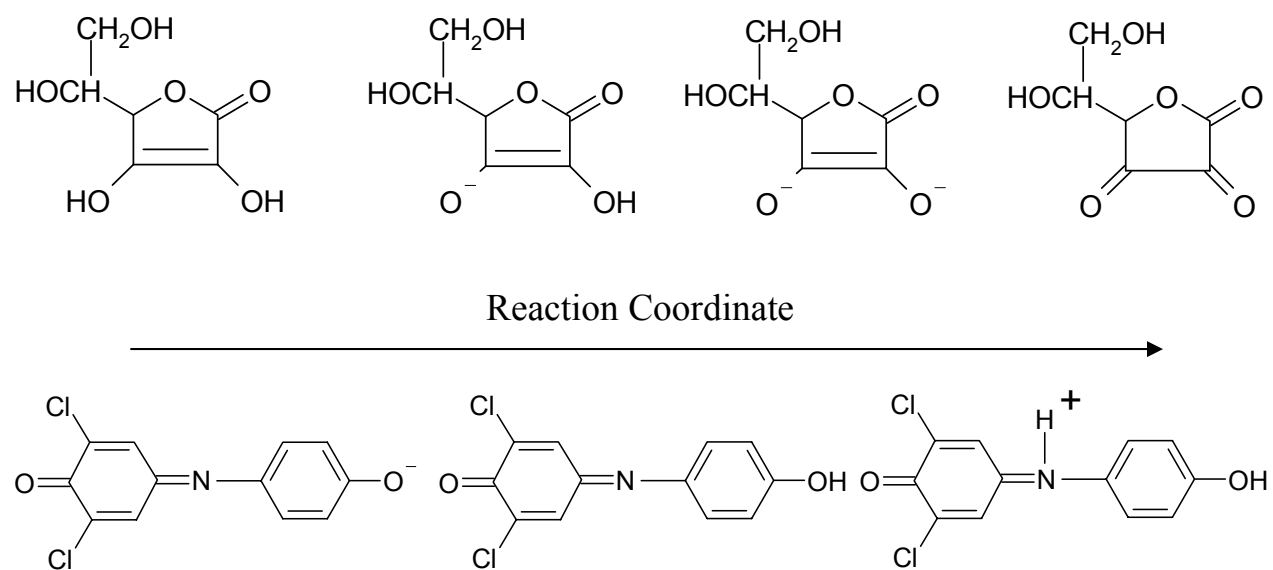


Figure 2.1: Ascorbic acid oxidation and subsequent reduction of DCIP. This reaction is monitored by a loss of absorbance at 420nm as the reaction proceeds.

Although the reaction rates seen with these reactions is much slower than those seen in diffusion-limited reactions, we needed a well behaved and well characterized reaction to determine proper functioning of the equipment in microgravity.

Materials and Methods

Cart Design: This section will describe the steps taken to adapt an ISS Koala spectrofluorometer and a Bio-Logic SFM 3 stopped-flow into a “mobile laboratory” in preparation for microgravity parabolic flights. Modification and testing of this equipment package was carried out predominantly by myself and Jason Bell in the LiCata lab at Louisiana State University. Stringent requirements for equipment durability and load bearing, provided by the NASA KC-135 flight operators, served as the starting point for our design. The equipment was contained in two carts, one containing the majority of necessary equipment, and one that served as a “work-bench.” (Figures 2.2 and 2.5)

A large, wheel mounted, steel cart (30” X 36” X 30.5”) served as the main chassis for Cart #1. This cart houses most of the major stopped-flow and fluorometer components, including most of the sensitive electronics shown in Figure 2.4. An ISS Koala fluorometer was attached to the top of the cart using the foot holes, normally used to attach the instrument to an optical bench. The ISS fluorometer was chosen for its modular design, which allows for easy manipulation of the photo-multiplier tubes and LED light sources. The cart was designed to accommodate an in-line absorbance mode, along with the standard fluorescence set-up.

A squared hole was also cut into the top of the cart, in order to accommodate the stopped-flow tower. This allowed for successful integration of the stopped flow components with the fluorometer. The top of the cart was supported with 3/4” multi-



Figure 2.2: Fully assembled Cart #1. Visible in this representation are the fluorometer (horizontally oriented black box, sitting on top of the steel cart), the SFM-3 stopped flow (vertically oriented black box in the “center” of the cart), the data collection computer (right side, black), the PX01 photon counting electronics (white vertical tower, right side), the electronic controller for the SFM stepping motors (white vertical tower, left side), and the UPS units (next to controller, left side.) Also visible is grey padding, used as needed, and the cargo straps which served as the main support for most components. A lab-jack supporting the SFM-3 is also visible.

layer plywood, to help accommodate the weight of the SFM-3. (Figure 2.2 and 2.3) The associated electronics were integrated into the cart, and attached with multiple cargo straps hooking to “U” bolts fastened to the walls of the cart. Appropriate foam padding was used, to protect the components from excessive shock they might experience upon flight take off and landing. Finally, a power surge protector was attached to the outside of the cart, to be used as a central “off” switch (Figure 2.4), and handles were attached to the cart.

Each of the electronic components was connected as they would be in a normal laboratory environment, however, running the necessary wires was logistically challenging. Figure 2.3 shows the rear view of Cart #1 in “fluorescence” mode. This picture illustrates the complexity of the wiring system, as each component’s connectors were routed through the same small port in the rear of the cart.

Cart #2 (Figure 2.5) was constructed upon a rubber cart, and contained the computer’s monitor, trackball mouse, and keyboard, as well as a Thermotek solid-state waterbath used for temperature regulation of the SFM-3. This cart acted as a “workbench” while on-board. The various computer components were attached with industrial-strength Velcro, and the monitor was additionally attached using cargo-straps bolted to the cart’s chassis. The water bath was attached to the cart via multiple cargo-straps.

All individual components and various component groups were tested for their ability to withstand g-force accelerations of between 2-9g in all directions. Testing was performed in a simplified manner by pulling on each component with a static force corresponding to 2-9 times that components weight.



Figure 2.3: Rear view of Cart #1 in the foreground, with Cart #2 in the distance. Visible in this picture is the complex nature of the connections between the instruments and their associated components housed “inside” the cart. All connections to the component systems were run through the small port in the rear of the cart. Additionally, this view clearly illustrates the modular nature of the ISS Koala spectrofluorometer, as the photomultiplier tubes are visible on either side of the fluorometer housing with the monochromator and LED connected at the rear. Each of these components could be configured to allow any arrangement necessary.

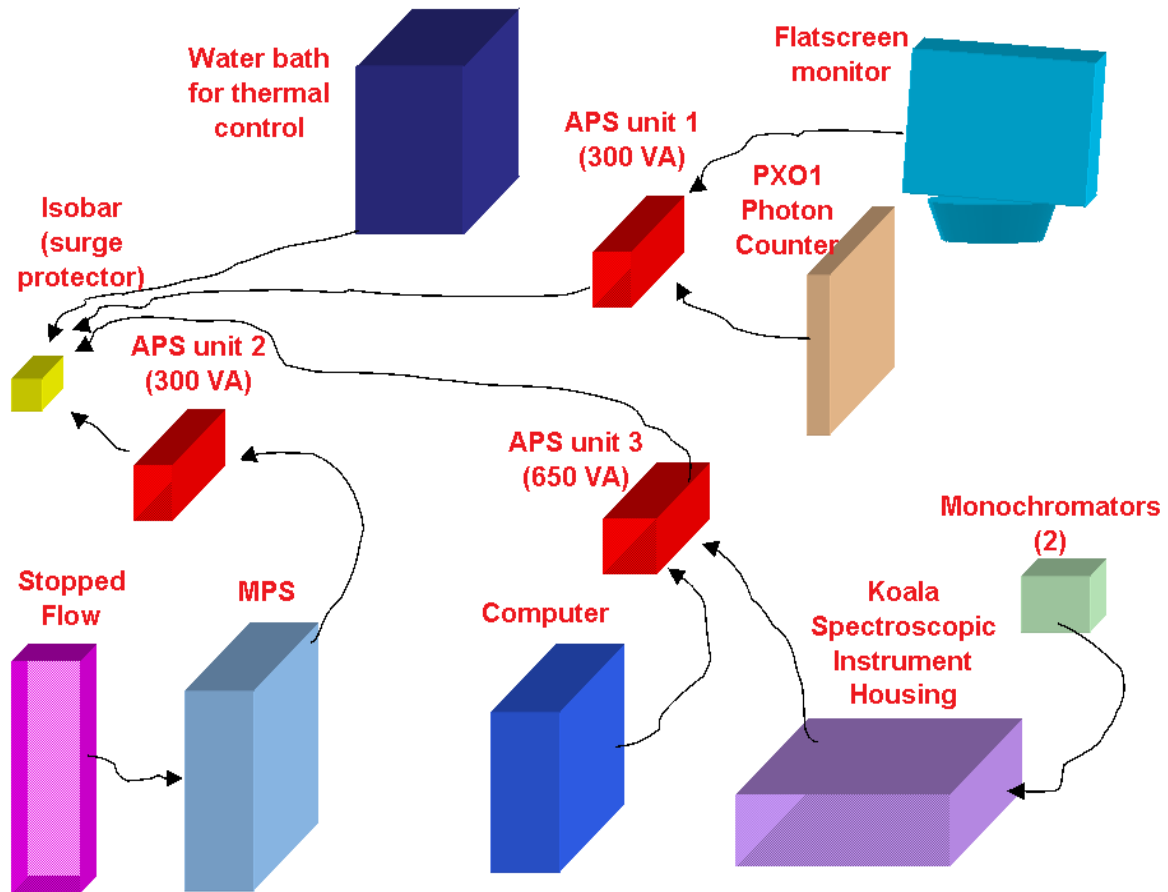


Figure 2.4: Schematic showing the electrical connection of the various components housed on the two carts. There are three APS devices, used to supply the instruments with uninterrupted power during potential brief moments of power loss. (APS #1-3) The components (starting in the lower left and moving counterclockwise) include: 1) The SFM-3 Stopped Flow is plugged directly into the MPS Stopped Flow Command Module. All of the components that drive the stopped-flows stepping motors are housed in the MPS. Additionally, the MPS powers the stopped-flow device. The MPS is plugged into APS #1, which is plugged into the Isobar 6-plug surge protecting power strip. 2) The monochromator assemblies are plugged directly into the Koala Spectroscopic Housing, which provides their power. The Koala Spectrophotometer and the computer are both plugged into APS #2, which was then plugged into the Isobar. 3) The computer monitor and photon counting electronics (PX01) are plugged into APS #3, which was plugged into the Isobar. 4) The Thermotek solid state water bath is plugged directly into the Isobar. The isobar was plugged into the aircraft power distribution panel. In addition to being a localized place for all components to plug into, the Isobar also serves as an emergency kill switch for power from the plane.



Figure 2.5: Fully assembled Cart #2. Visible in this picture are the Thermotek water-bath (left-side of the cart, attached with an orange cargo strap), the computer's monitor, keyboard, and track-ball mouse. Cargo straps and industrial grade Velcro were used to attach the various components.

DCIP and Ascorbic Acid Reactions: DCIP was prepared at 140uM in water. In all experiments, the concentration of DCIP used was 140uM. Ascorbic acid was prepared in water and pH'd using concentrated NaOH or HCl. Different concentrations of Ascorbic acid were achieved by mixing (in the stopped-flow), a low and a high concentration solution, in appropriate volumes before mixing with DCIP.

Data Analysis: Kinetic traces were fit to single exponential equations. (Equation 2.1) In all cases tested, a double exponential fit did not improve the fit.

$$Y = Y_0 + A_1 e^{-(x-x_0)/\tau}$$

(Equation 2.1)

All reactions were all performed under pseudo-first order conditions. The rate of a pseudo-first order reaction is determined by monitoring the k_{obs} or $1/\tau$ with respect to concentration of a variable reactant (Hammes, 2000). The first-order rate (k_1) is proportional to the slope of this relationship (Equation 2.2).

$$k_{obs} = 1/\tau = k_1[A]_0$$

(Equation 2.2)

A plot of k_{obs} vs. [ascorbic acid] yields a straight line, with a y-intercept of zero under perfect conditions. However, because small errors in k_{obs} can lead to very large errors in the y-intercept, the data were fit in various ways. In addition to fitting the data

to Equation 2.2, another fitting option was exercised. In some cases, as noted, data was fit to Equation 2.3, with a floating y-intercept term, k_{-1} .

$$1 / \tau = k_1 [A]_0 + k_{-1}$$

(Equation 2.3)

Results and Discussion

“In-Lab” Reaction Characterization: The DCIP and ascorbic acid reaction was carried out under “normal” lab conditions in order to determine the fastest reaction that could be easily monitored at 25°C. As mentioned above, the reaction rate is very pH sensitive, with the more rapid reaction occurring at lower pH. In order to determine which pH was most amenable to on-board reaction conditions, the rate profile of the reaction was measured at pH 5, pH 6, and pH 9. Figure 2.6 shows the k_{obs} measured at varying ascorbic acid concentration at three pHs, as mentioned. The most rapid reaction which could be measured with high reproducibility was determined to be pH 6, while pH 9 was well behaved over multiple attempts, as well. The k_1 (determined by fit to Equation 2.2) measured was $5441 \pm 173 \text{ M}^{-1}\text{sec}^{-1}$ at pH 5, $734 \pm 17 \text{ M}^{-1}\text{sec}^{-1}$ at pH 6, and $256 \pm 3 \text{ M}^{-1}\text{sec}^{-1}$ at pH 9. As expected the lower pH reactions occurred much more rapidly than the pH 9 reactions. While our goal was to measure the most rapid reaction onboard the aircraft, the pH 5 reactions contained too much error to be able to measure the reaction with high precision. Further, when the pH 5 data was fit to Equation 2.3, the errors in k_{obs} translated into a dramatic deviation of the y-intercept term from 0. Indeed, very small errors in the measured k_{obs} can translate into proportionally larger deviations from a y-intercept of zero.

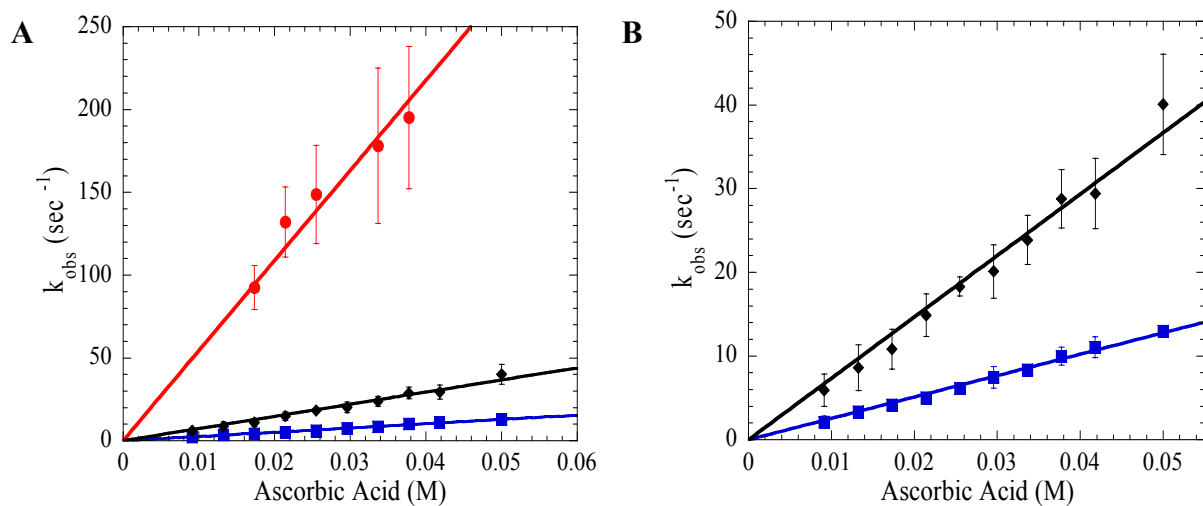


Figure 2.6: Panel A: k_{obs} vs. Ascorbic acid measured in-lab at varying pH. pH 5 (red circles), pH 6 (black diamonds), and pH 9 (blue squares), fit to equation 2.2. Error bars represent the standard deviation of multiple measurements. **Panel B:** pH 6 and pH 9 data from Panel A graphed on a different scale.

Reactions at pH 6 and pH 9 were chosen as appropriate for the onboard reactions. Believing that rapid reactions might show a more dramatic effect under microgravity, pH 6 was chosen as the “focus” of the flights.

“In-Flight” Experiments, pH 6: This section describes the results measured onboard the KC-135 Reduced Gravity Laboratory. All reactions were measured on-board the aircraft either before microgravity parabolic maneuvers began, or under microgravity, as noted.

Given the extreme conditions of the KC-135 flights, it was necessary to determine whether data collected under microgravity conditions was of the same quality as that measured under normal gravity conditions. Figure 2.7, Panel A shows the reaction measured at pH 6 under normal gravity, while Panel B shows the same reaction measured during a single period of microgravity. Each trace was generated from an average of 3 shots collected at identical concentrations. It was determined that the quality of the data collected under microgravity was comparable to data collected during the onboard control.

A full series of reactions was collected on-board at varying concentrations of ascorbic acid, under 1g gravity conditions and during periods of microgravity. The full series of data was collected and averaged, then fit to Equation 2.1, to determine the microscopic rate constant, k_{obs} . In all cases, at least 3 shots were collected and averaged. A plot of k_{obs} vs. [ascorbic acid] yields a linear relationship under all conditions measured. These data sets were fit in two ways. Initially, the data was fit to Equation 2.2 in order to determine the pseudo-first order rate (k_1) of $850 \pm 43 \text{ M}^{-1}\text{sec}^{-1}$ under 1g onboard control conditions, and $852 \pm 36 \text{ M}^{-1}\text{sec}^{-1}$ under microgravity. (Figure 2.8)

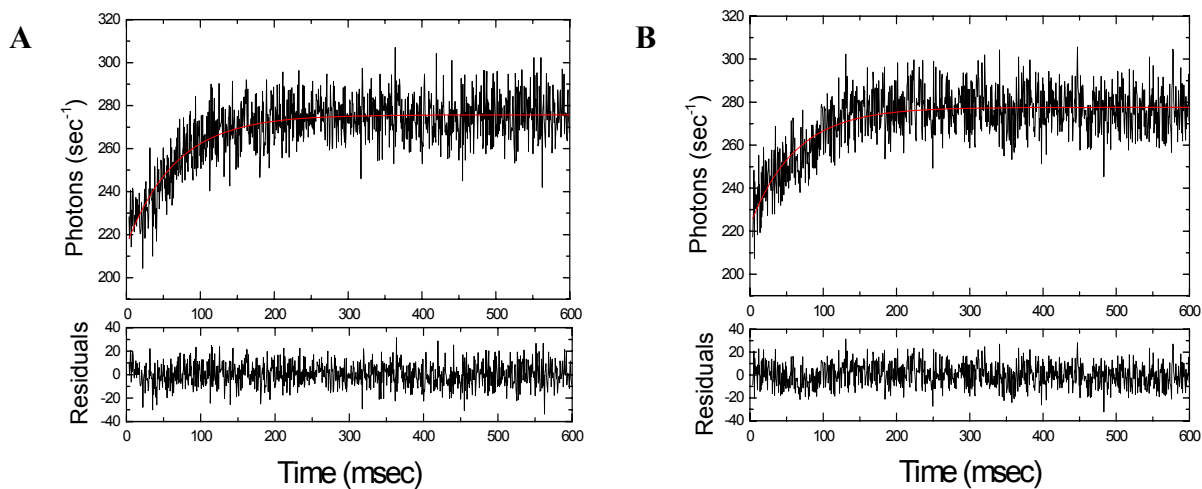


Figure 2.7: Representative curves collected while onboard KC-135 flights. An average of 3 independent shots of 21.42mM ascorbic acid (pH 6) into DCIP was used for each trace represented above. **Panel A** shows the shots collected during the on-board control. **Panel B** shows the data collected while under microgravity. Curves were fit to Equation 2.1, and the residuals to the fit are shown below each curve.

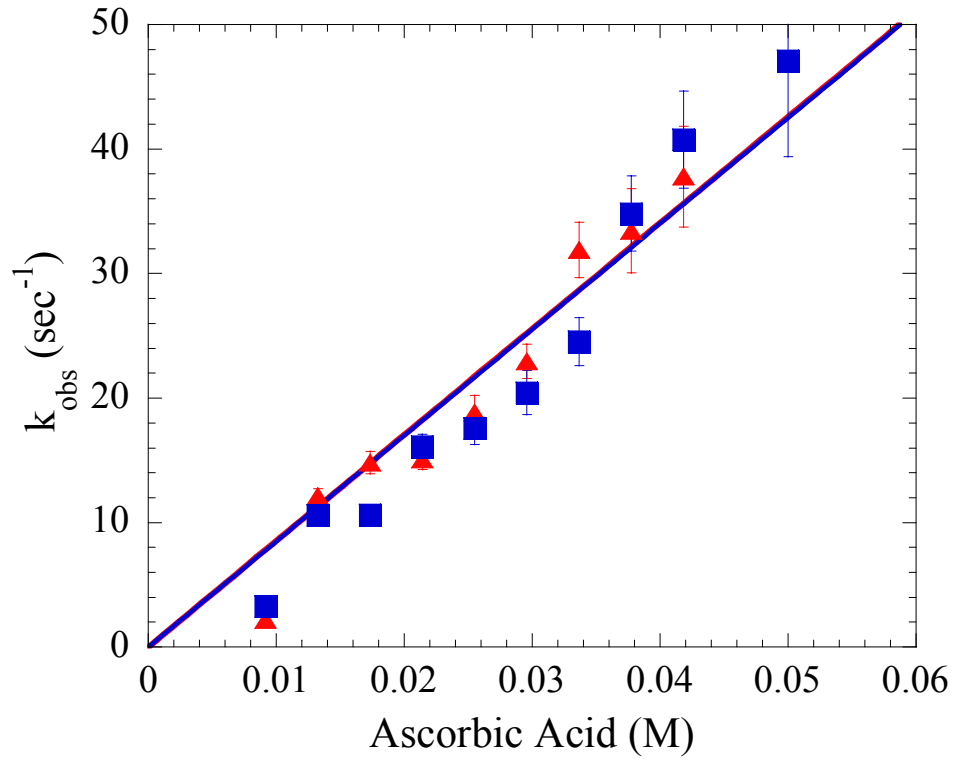


Figure 2.8: k_{obs} vs. [ascorbic acid] series measured under microgravity (red triangles) and under normal gravity (blue squares) collected onboard KC-135 flights. The lines represent best fits of data sets to Equation 2.2.

Additionally, the data sets were fit to Equation 2.3. This analysis was performed in order to obtain some understanding of the error present in our data. Data collected under perfect lab conditions should have an invariant k_1 when fit to either Equation 2.2 or Equation 2.3, and each analysis should produce a y-intercept value of 0. Any deviation from that standard is probably due to systematic error in our onboard system. Fitting our data sets to Equation 2.3 (Figure 2.9) revealed a k_1 of $1066 \pm 75 \text{ M}^{-1}\text{sec}^{-1}$ with an intercept of -7 sec^{-1} under normal gravity, and $1014 \pm 77 \text{ M}^{-1}\text{sec}^{-1}$ with an intercept of -5 sec^{-1} under microgravity.

Regardless of the fitting technique used, there does not seem to be any significant change in the reaction rate (k_1) from the control under microgravity. Given the difference between the fits to the two equations, we can determine that our system contains some systematic error, as data collected in the laboratory (Figure 2.6) did not show this behavior. These results were not completely surprising, given the extreme conditions which exist on-board the aircraft. In addition to the microgravity conditions, purposely introduced, there are a number of other significant deviations from “normal” lab conditions. Conditions beyond our control included; significant aircraft vibration, occasional loss of temperature control, and highly unregulated ambient temperatures, which fluctuated between 20°C and 30°C . Each of these conditions probably contributed to this non-ideality. Interestingly, however, any deviation from the best fit to Equation 2.2 seen in one condition was mimicked in the other.

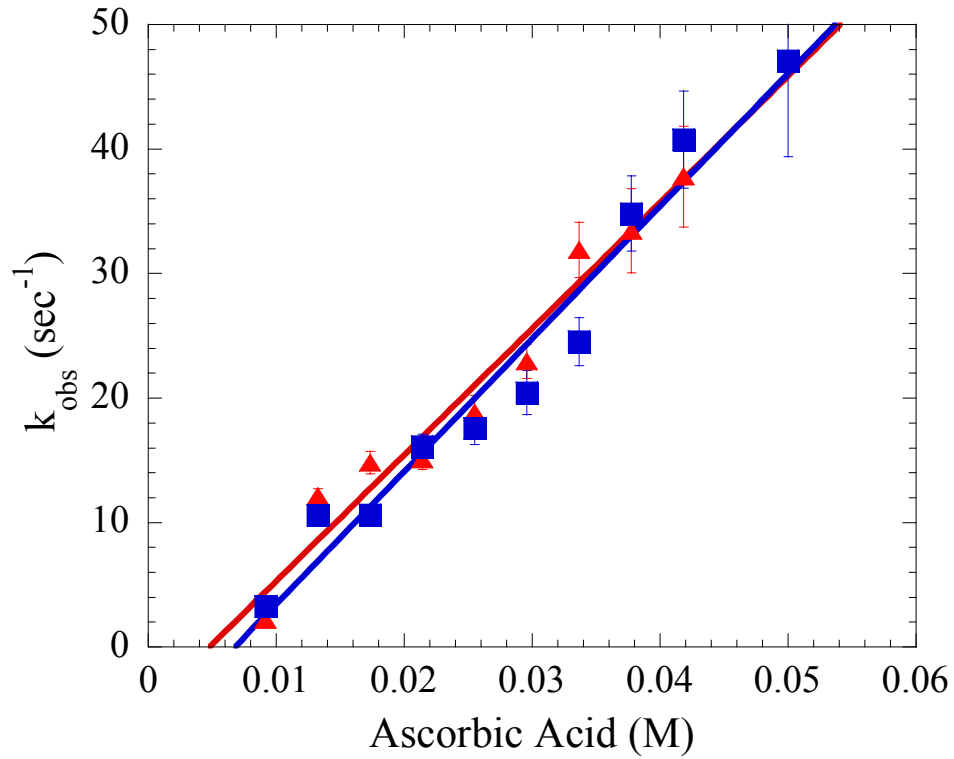


Figure 2.9: k_{obs} vs. [ascorbic acid] series measured under microgravity (red triangles) and under normal gravity (blue squares) collected onboard KC-135 flights. The lines represent best fits of data sets to Equation 2.3.

“In-Flight” Experiments, pH 9: A reaction series was also collected at pH 9 under microgravity. However, due to lack of time, an onboard control could not be performed. The microgravity data collected onboard was plotted and fit to Equations 2.2 and 2.3. As a control, the data was plotted against the in-lab control reactions (Figures 2.10 and 2.11). While this control is not ideal, it is a very well characterized reaction of 10 replicates per ascorbate concentration, and only small changes in reaction rate were noted between the microgravity and ground control series. Therefore, we believe this to be a valid control reaction, measured without the added systematic error introduced onboard the aircraft.

The pH 9 data series collected on-board is clearly not as well behaved as the control collected in the lab. When data series are fit to Equation 2.2 to determine the k_1 , the 1g lab control yielded a k_1 of $256 \pm 3 \text{ M}^{-1}\text{sec}^{-1}$, while the rate determined under microgravity was $283 \pm 23 \text{ M}^{-1}\text{sec}^{-1}$. While there is a small change in the rate measured onboard, the random and systematic error present in the system prohibits definitive comparison of the two data sets.

The k_1 measured for pH 9 in the lab, when fit to Equation 2.3, was found to be $271 \pm 6 \text{ M}^{-1}\text{sec}^{-1}$, with an intercept value of -0.5 sec^{-1} . While the reaction series measured under microgravity conditions was determined to be $387 \pm 40 \text{ M}^{-1}\text{sec}^{-1}$ with an intercept value of -4 sec^{-1} . While this seems to be a significant change in k_1 , the results should only be interpreted as interesting, given the lack of an onboard control, and the relative volatility of the k_{obs} 's measured under microgravity.

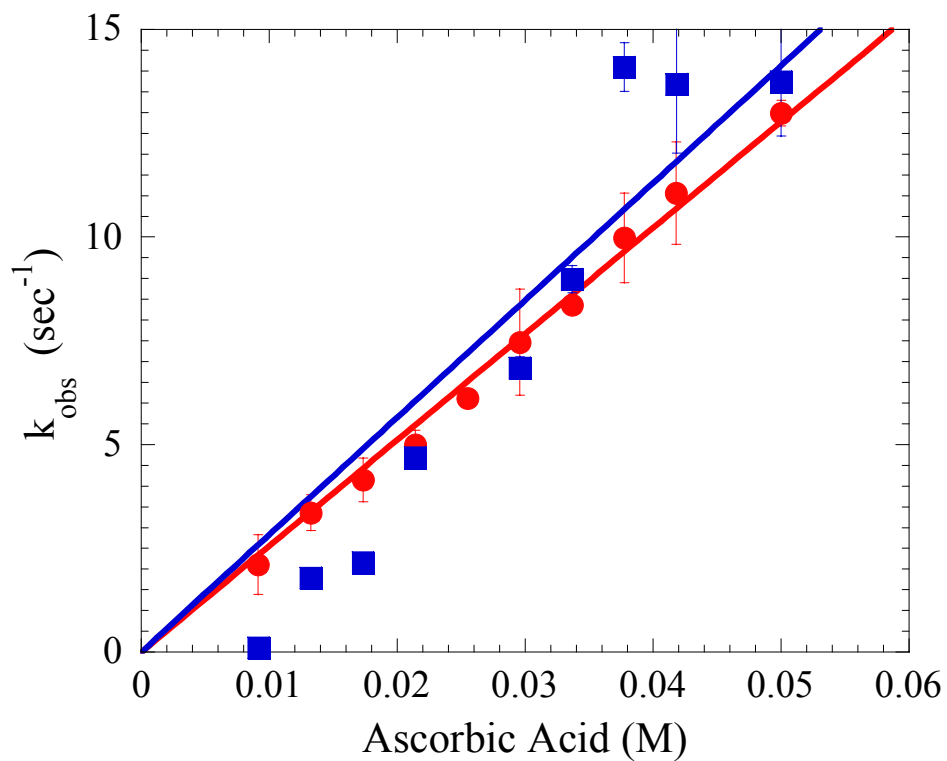


Figure 2.10: k_{obs} vs. [ascorbic acid] reaction series at pH 9, collected in lab (red circles) and onboard (blue squares) the KC-135 during periods of microgravity. Lines represent best fits to Equation 2.2.

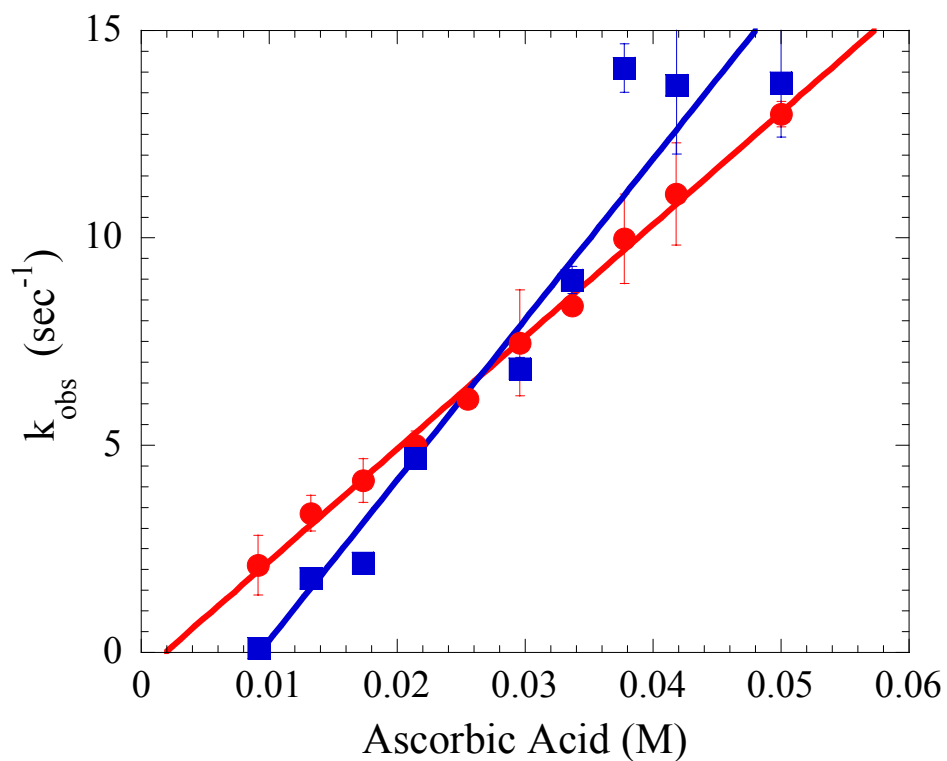


Figure 2.11: k_{obs} vs. [ascorbic acid] reaction series at pH 9, collected in lab (red circles) and onboard (blue squares) the KC-135 during periods of microgravity. Lines represent best fits to Equation 2.3.

Conclusions

The goals of this project were to assemble a mobile rapid kinetics laboratory for use onboard NASA's KC-135 microgravity airplane, and to determine if there is any change in the rate of a small molecule reaction in the presence of microgravity vs. a 1g control. The DCIP reduction reactions did not show any gravity dependence. This result was not unexpected, as the reactions measured here are significantly (10^4 - 10^6) slower than diffusion controlled reactions (Cantor and Schimmel, 1980), which we hypothesize will be most affected by microgravity.

Though no change in the rate of DCIP reduction was seen, many successes are documented here. The proper functioning of the instruments under the extreme environment of microgravity was very heartening. Many technical challenges were addressed to allow these experiments. The carts, as assembled, will only require minor changes in preparation for future flights. Future flights will determine the gravity effects on extremely rapid, diffusion limited, protein-ligand interactions.

References

- Graebe, A., Schuck, E. L., Lensing, P., Putcha, L., and Derendorf, H. (2004) Physiological, Pharmacokinetic, and Pharmacodynamic Change in Space. *J. Clin. Pharmacol.* **44(8)**: 837-853.
- Cantor, C. R. and Schimmel, P. R. (1980) Biophysical Chemistry, Part III, The Behavior of Biological Macromolecules. W. H. Freeman and Company. San Francisco, CA. USA.
- Hammes, G. G. (2000) Thermodynamics and Kinetics for the Biological Sciences. A. J. Wiley and Sons. New York, NY. USA.
- Maccarrone, M., Tacconi, M., Battista, N., Valgattari, F., Falciani, P., Finazzi-Agro, A. (2001) Lipoxygenase Activity During Parabolic Flights. *J. Gravit. Physiol.* **8 (1)**: 123-124.

Nickerson, C. A., Ott, C. M., Wilsion, J. W., Ramamurthy, R., and Pierson, D., L. (2004) Microbiological Responses to Microgravity and Other Low-Shear Environments. *Microbiol. Mol. Rev. Biol. Rev.* **68 (2)**: 345-361.

Ohnishi, T., Takahashi, A., Ohnishi, K., Nakano, T., and Nagaoka, S. (2000) Enzymic Chemical Reaction Under Microgravity Environment in Space. *J. Gravit. Physiol.* **7 (2)**: 69-70.

Papaseit, C., Pochon, N., and Tabony, J. (2000) Microtubule Self-Organization is Gravity-Depended. *Proc. Natl. Acad. Sci. U. S. A.* **97 (15)**: 8364-8368.

Ranaldi, F., Vanni, P., and Giachetti, E. (2003) Enzyme Catalysis in Microgravity: Steady-State Kinetic Analysis of the Isocitrate Lyase Reaction. *Biophysical Chemistry.* **103 (2)**: 169-177.

Tonomura, B., Nakatani, H., Ohnishi, M., Yamaguchi-Ito, J., and Hiromi, K. (1978) Test Reactions for a Stopped-Flow Apparatus: Reduction of 2, 6-Dichlorophenolindophenol and Potassium Ferricyanide by L-Ascorbic Acid. *Anal. Biochem.* **84**: 370-383.

Walther, I., Pippia, P., Meloni, M. A., Turrini, F., Mannu, F., and Cogoli, A. (1998) Simulated Microgravity Inhibits the Genetic Expression of Interleukin-2 and its Receptor in Mitogen-Activated T Lymphocytes. *F. E. B. S. Letters.* **(436)**: 115-118.

APPENDIX 1

OLIGONUCLEOTIDE PRIMERS USED

This appendix lists the primers used in this thesis, and contains a brief description of each.

1707Nco and 1707Bam2 were used to amplify the full-length *D. radiodurans* polymerase from amplified genomic material provided by John Battista (Louisiana State University). 1707Nco introduced an NcoI site at the N-terminus of the gene. An NcoI cutsite contains the sequence for an N-terminal methionine start site. 1707Bam2 contained the sequence for a BamHI cutsite, introduced at the C-terminus of the gene. These cutsites were used to introduce the gene into the pET15b vector. Their sequences are:

1707Nco: 5'-GGGCTCCTTTTCCATGGTTTTTTGTGGTGA-3'

1707Bam2: 5'-CAGTACGCCGGGATCCTCGCCCCCTCACTTC-3'

KDNcoI-2 and 1707Bam2 were used to amplify the large fragment Klendein gene from the full length plasmid. 1707Bam2 is described above. KDNcoI-2 was used to introduce an NcoI cutsite at the N-terminus of the Klendein gene. This cutsite contains the codon for an N-terminal methionine start site.

KDNcoI-2: 5'-GAACACGCGCAGACCCATGGGAGGAGGACGAGG-3'

The following oligonucleotide primers were used in sequencing reactions to confirm the sequences of all plasmids used:

SP1707-8: 5'-TTTGTGGTGACGGTGGTCTGTC-3'

SP1707-563: 5'-TGAACCTCATCGCCAACGAC-3'

SP1707-979: 5'-TGAACGGGCCAGAACAGGAATGG-3'

SP1707-1280: 5'-TGCCGAGCGACAAACCATTG-3'

SP1707-1840: 5'-CAGCTCGAAACGGTGCTTTACG-3'

SP1707-2380: 5'-TGCTGTACGGCATGAGTGCTC-3'

RP1707-351: 5'-CGACTTGTAGCCCTCGTACTG-3'

Primers denoted SP1707 are primers used for “forward” sequencing. The number denotes the position of the 5' end of the primer. Each primer was used to sequence approximately 800 bases. Primers were designed to allow for ~100-200 basepair overlaps between primers. Primer RP1707-351 is a “reverse” primer, designed to sequence the primer in the reverse direction to sequence bases missed by the earliest downstream primers.

The following mutagenic primers were used for site-directed mutagenesis of positions 412 and 757.

G412A: 5'-CGAGCCCGACGAGTGGGGGCAGGC-3'

G412A-R: 5'-GCCTGCGCCCACTCGTCTGGGCTCG-3'

C757T: 5'-ATGCAGCAGGCGTTCGTGGAGGGTGC-3'

C757T-R: 5'-GCACCCTCCACGAACGCCTGCTG-3'

APPENDIX 2

SEQUENCE ALIGNMENTS

Full sequence alignments of *E. coli* pol I, *T. aquaticus* pol I, *D. radiodurans* pol I, Klenow, Klentaq, and Klendein.

```

E. coli pol I      - - - - -
T. aquaticus pol I - - - - - MR GML
D. radiodurans pol I MVF C G D G G L S C E S I D F A L C C L R G R S G N Y V Q S R I L P M A D A S
Klenow            - - - - -
Klentaq           - - - - -
Klendein         - - - - -

E. coli pol I      MVQ I P Q N P L I L V D G S S Y L Y R A Y H A F P P L T N S A G E P T G A M Y
T. aquaticus pol I P L F E P K G R V L L V D G H H L A Y R T F H A L K G L T T S R G E P V Q A V Y
D. radiodurans pol I P D P S K P D T L V L I D G H A L A F R S Y F A L P P L N N S K G E M T H A I V
Klenow            - - - - -
Klentaq           - - - - -
Klendein         - - - - -

E. coli pol I      G V L N M L R S L I M Q Y K P T H A A V V F D A K G K T F R D E L F E H Y K S H
T. aquaticus pol I G F A K S L L K A L K E D G - D A V I V V F D A K A P S F R H E A Y G G Y K A G
D. radiodurans pol I G F M K L L L R L A R Q K S - N Q V I V V F D P P V K T F R H E Q Y E G Y K S G
Klenow            - - - - -
Klentaq           - - - - -
Klendein         - - - - -

E. coli pol I      R P P M P D D L R A Q I E P L H A M V K A M G L P L L A V S G V E A D D V I G T
T. aquaticus pol I R A P T P E D F P R Q L A L I K E L V D L L G L A R L E V P G Y E A D D V L A S
D. radiodurans pol I R A Q T P E D L P G Q I N R I R A L V D A L G F P R L E E P G Y E A D D V I A S
Klenow            - - - - -
Klentaq           - - - - -
Klendein         - - - - -

E. coli pol I      L A R E A E K A G R P V L I S T G D K D M A Q L V T P N I T L I N T M T N T I L
T. aquaticus pol I L A K K A E K E G Y E V R I L T A D K D L Y Q L L S D R I H V L H P E G - Y L I
D. radiodurans pol I L T R M A E G K G Y E V R I V T S D R D A Y Q L L D E H V K V I A N D F - S L I
Klenow            - - - - -
Klentaq           - - - - -
Klendein         - - - - -

E. coli pol I      G P E E V V N K Y G V P P E L I I D F L A L M G D S S D N I P G V P G V G E K T
T. aquaticus pol I T P A W L W E K Y G L R P D Q W A D Y R A L T G D E S D N L P G V K G I G E K T
D. radiodurans pol I G P A Q V E E K Y G V T V R Q W V D Y R A L T G D A S D N I P G A K G I G P K T
Klenow            - - - - -
Klentaq           - - - - -
Klendein         - - - - -

E. coli pol I      A Q A L L Q G L G G L D T L Y A E P E K I A G L S F R G A K T M A A K L E Q N K
T. aquaticus pol I A R K L L E E W G S L E A L L K N L D R - - - L K P A I R E K I L A H M D D L K
D. radiodurans pol I A A K L L Q E Y G T L E K V Y E A A H A G T L K P D G T R K K L L D S E E N V K
Klenow            - - - - -
Klentaq           - - - - -
Klendein         - - - - -

E. coli pol I      E V A Y L S Y Q L A T I K T D V E L E L T C E Q L E V Q Q P A A E E L L G L F K
T. aquaticus pol I L S W D L A K V R T D L P L E V D F A K R R E P D R E R L R A F L E R L - - - -
D. radiodurans pol I F S H D L S C M V T D L P L D I E F G V R R L P D N P L V T E D L L T E - - - -

```

```

Klenow      - - - - -
Klentaq    - - - - -
Klendeim   - - - - -

E. coli pol I  KYEFKRWTADVEAGKWLQAKGAKPAAKPQETSVADEAPEV
T. aquaticus pol I  - - - - - EFGSLH - - - - -
D. radiodurans pol I  - - - - - LELHSLRPMILGLNGPEQDGHAPDDLLEHA
Klenow      - - - - -
Klentaq    - - - - -
Klendeim   - - - - -

E. coli pol I  TATVISYDNYVTILDEETLKAWIAKLEKAPVFAFDTETDS
T. aquaticus pol I  - - - - - EFGLLLESPKALEEAPWP-PPEGA-FVGFVLSRK-
D. radiodurans pol I  QTPEEDEAAALPAFSAPELAEWQTPAEGA-VWGYVLSRE-
Klenow      - - - - - VISYDNYVTILDEETLKAWIAKLEKAPVFAFDTETDS
Klentaq    - - - - - -MSPKALEEAPWP-PPEGA-FVGFVLSRK-
Klendeim   - - - - - -MAFSAPELAEWQTPAEGA-VWGYVLSRE-

E. coli pol I  LDNISANLVGLSFAIEP GVAAYIPVAHDYLDAPDQISRER
T. aquaticus pol I  - EPMWADLLALAAARG-GRVHRAPEP- - - - -
D. radiodurans pol I  - DDLTAAALLAAATFED- GVARPAPVSEPDEWAQAEAPENL
Klenow      LDNISANLVGLSFAIEP GVAAYIPVAHDYLDAPDQISRER
Klentaq    - EPMWADLLALAAARG-GRVHRAPEP- - - - -
Klendeim   - DDLTAAALLAAATFED- GVARPAPVSEPDEWAQAEAPENL

E. coli pol I  ALELLKP - - - - - LLEDEKALKVGNLKYDRGILAN - - - - -
T. aquaticus pol I  - - - - - - - - - - YKALRDLKEARGLL - - - - -
D. radiodurans pol I  FGELLP SDKPLTKK EQKALEKAQKDAEKARAKLREQFPAT
Klenow      ALELLKP - - - - - LLEDEKALKVGNLKYDRGILAN - - - - -
Klentaq    - - - - - - - - - - YKALRDLKEARGLL - - - - -
Klendeim   FGELLP SDKPLTKK EQKALEKAQKDAEKARAKLREQFPAT

E. coli pol I  - - - - - YGIELRGI AFDTMLESYILNSVAGRHDMDSLA
T. aquaticus pol I  - - - - - - - - - - AKDLSVLALREGLGLPPGDDPMLL
D. radiodurans pol I  VDEAEFVQGRTVTAAA AKALAAHLSVRGT VVEPGDDPPLY
Klenow      - - - - - YGIELRGI AFDTMLESYILNSVAGRHDMDSLA
Klentaq    - - - - - - - - - - AKDLSVLALREGLGLPPGDDPMLL
Klendeim   VDEAEFVQGRTVTAAA AKALAAHLSVRGT VVEPGDDPPLY

E. coli pol I  ERWLKHKTI TFE E IAGKGKNQLTFNQIALEBAGRYAAEDA
T. aquaticus pol I  AYLLDP SNTTPEGVARR - - - - - YGG-EWTEBAGERA
D. radiodurans pol I  AYLLDP ANT NMPVVAKR - - - - - YLDREWPADAPTRA
Klenow      ERWLKHKTI TFE E IAGKGKNQLTFNQIALEBAGRYAAEDA
Klentaq    AYLLDP SNTTPEGVARR - - - - - YGG-EWTEBAGERA
Klendeim   AYLLDP ANT NMPVVAKR - - - - - YLDREWPADAPTRA

E. coli pol I  DVTLQLHLKMWPD LQKHKGPLENVFENIEMPLVPVLSRIER
T. aquaticus pol I  ALSERL FANLWGRLEGEERLLWL YREVERPLSAVLAHMEA
D. radiodurans pol I  AITGHL LREL PPLDDARR - - KMYDEMEKPLSGVLGRMEV
Klenow      DVTLQLHLKMWPD LQKHKGPLENVFENIEMPLVPVLSRIER
Klentaq    ALSERL FANLWGRLEGEERLLWL YREVERPLSAVLAHMEA
Klendeim   AITGHL LREL PPLDDARR - - KMYDEMEKPLSGVLGRMEV

```

E. coli pol I NGVKIDPKV LHNHSE ELTLRLAE LEKKAHEI AGE EFNLS S
T. aquaticus pol I TGVRLDVAYLRALS LEVAEEIARLEAEVFR LAGHPFNLS S
D. radiodurans pol I RGVQVDSDFLQTL SIQAGVRLADLESQI HEYAGEEFHIRS
 Klenow NGVKIDPKV LHNHSE ELTLRLAE LEKKAHEI AGE EFNLS S
 Klentaq TGVRLDVAYLRALS LEVAEEIARLEAEVFR LAGHPFNLS S
 Klendeim RGVQVDSDFLQTL SIQAGVRLADLESQI HEYAGEEFHIRS

E. coli pol I TKQLQTI LFEKQGIKPLKKT PG - GAPSTSEE VLEELALDY
T. aquaticus pol I RDQLERVLFDELGLPAIGKTEKTGKRSTSAAVLEALREAH
D. radiodurans pol I PKQLETVLYDKLELASSKKTCLTGQRSTAVSALEPLRDAH
 Klenow TKQLQTI LFEKQGIKPLKKT PG - GAPSTSEE VLEELALDY
 Klentaq RDQLERVLFDELGLPAIGKTEKTGKRSTSAAVLEALREAH
 Klendeim PKQLETVLYDKLELASSKKTCLTGQRSTAVSALEPLRDAH

E. coli pol I PLPKVILEYRGLAKLKSTYT DKLPLMINPKTGRVHTSYHQ
T. aquaticus pol I PIVEKILQYRELTKLKSTYIDPLPDLIHPRTGRLHTRFNQ
D. radiodurans pol I PIIPLVLEFRELDKLRGTYLDPIPNLVNPHHTGRLHTTFAHQ
 Klenow PLPKVILEYRGLAKLKSTYT DKLPLMINPKTGRVHTSYHQ
 Klentaq PIVEKILQYRELTKLKSTYIDPLPDLIHPRTGRLHTRFNQ
 Klendeim PIIPLVLEFRELDKLRGTYLDPIPNLVNPHHTGRLHTTFAHQ

E. coli pol I AVTATGRLSS TDPNLQNI PVRNE EGRRIRQAFIAPEDYVI
T. aquaticus pol I TATATGRLSS SDPNLQNI PVRTPLGQRIRRAFIAEEGWLL
D. radiodurans pol I TAVATGRLSS LNPNLQNIPIRSELGREIRKGFIAEDGFTL
 Klenow AVTATGRLSS TDPNLQNI PVRNE EGRRIRQAFIAPEDYVI
 Klentaq TATATGRLSS SDPNLQNI PVRTPLGQRIRRAFIAEEGWLL
 Klendeim TAVATGRLSS LNPNLQNIPIRSELGREIRKGFIAEDGFTL

E. coli pol I VSADYSQIELRIMAHLSRDKGLLTAFAEGKDIHRATAAEV
T. aquaticus pol I VALDYSQIELRVLAHLSGDENLIRVFQEGRDIHTETA SWM
D. radiodurans pol I IAADYSQIELRLLAHIADDP LMQQAFVEGADIHRRTAAQV
 Klenow VSADYSQIELRIMAHLSRDKGLLTAFAEGKDIHRATAAEV
 Klentaq VALDYSQIELRVLAHLSGDENLIRVFQEGRDIHTETA SWM
 Klendeim IAADYSQIELRLLAHIADDP LMQQAFVEGADIHRRTAAQV

E. coli pol I FGLPLETVTSEQRSSAKA INFGVLIYGMSAFGLARQLNI PR
T. aquaticus pol I FGVPREAVDPLMRRRAAKTINFGVLYGMSAHRLSQBLAIPY
D. radiodurans pol I LGLDEATVDANQRRRAAKTVNFGVLYGMSAHRLSNDLGIPY
 Klenow FGLPLETVTSEQRSSAKA INFGVLIYGMSAFGLARQLNI PR
 Klentaq FGVPREAVDPLMRRRAAKTINFGVLYGMSAHRLSQBLAIPY
 Klendeim LGLDEATVDANQRRRAAKTVNFGVLYGMSAHRLSNDLGIPY

E. coli pol I KEAQKYMDLYFERYPGVLEYMERTRAQAKEQGYVETLDGR
T. aquaticus pol I EEAQAFIER YFQSFPKVRAWIEK TLEEGRRRGYVETL FGR
D. radiodurans pol I AEAATFIEIYFATYPGIRRYINH TLDFGRTHGYVETLYGR
 Klenow KEAQKYMDLYFERYPGVLEYMERTRAQAKEQGYVETLDGR
 Klentaq EEAQAFIER YFQSFPKVRAWIEK TLEEGRRRGYVETL FGR
 Klendeim AEAATFIEIYFATYPGIRRYINH TLDFGRTHGYVETLYGR

E. coli pol I RLYLPDIKSSNGARRAAAERAAI NAFMQGTAADI IKRAMI
T. aquaticus pol I RRYVPDLEARVKS VREAAERMAFNMPVQGTAADLMK LAMV

D. radiodurans pol I	R R Y V P G L S S R N R V Q R E A E E R L A Y N M P I Q G T A A D I M K L A M V
Klenow	R L Y L P D I K S S N G A R R A A A E R A A I N A P M Q G T A A D I I K R A M I
Klentaq	R R Y V P D L E A R V K S V R E A A E R M A F N M P V Q G T A A D L M K L A M V
Klendein	R R Y V P G L S S R N R V Q R E A E E R L A Y N M P I Q G T A A D I M K L A M V
E. coli pol I	A V D A W L Q A E Q P R V R M I M Q V H D E L V F E V H K D D V D A V A K Q I H
T. aquaticus pol I	K L F P R L E E M G - - A R M L L Q V H D E L V L E A P K E R A E A V A R L A K
D. radiodurans pol I	Q L D P Q L D A I G - - A R M L L Q V H D E L L I E A P L D K A E Q V A A L T K
Klenow	A V D A W L Q A E Q P R V R M I M Q V H D E L V F E V H K D D V D A V A K Q I H
Klentaq	K L F P R L E E M G - - A R M L L Q V H D E L V L E A P K E R A E A V A R L A K
Klendein	Q L D P Q L D A I G - - A R M L L Q V H D E L L I E A P L D K A E Q V A A L T K
E. coli pol I	Q L M E N C T R L D V P L L V E V G S G E N W D Q A H -
T. aquaticus pol I	E V M E G V Y P L A V P L E V E V G I G E D W L S A K E
D. radiodurans pol I	K V M E N V V Q L K V P L A V E V G T G P N W F D T K -
Klenow	Q L M E N C T R L D V P L L V E V G S G E N W D Q A H -
Klentaq	E V M E G V Y P L A V P L E V E V G I G E D W L S A K E
Klendein	K V M E N V V Q L K V P L A V E V G T G P N W F D T K -

APPENDIX 3

13/20MER BINDING IN KACETATE

Klenow and Klentaq binding 13/20mer DNA in varying KAcetate concentrations					
<i>Klenow</i>			<i>Klentaq</i>		
[KAcetate] (M)	K_d (nM)*	Linkage**	[KAcetate] (M)	K_d (nM)*	Linkage**
.3	5.1 ± 0.2		.1	12.1 ± 0.5	
.35	13.4 ± 0.74		.125	34.7 ± 1.2	
.4	17.1 ± 1.3	4.4 ± 0.4	.15	66.25 ± 2.6	3.8 ± 0.2
.45	35.93 ± 1.1		.175	95.9 ± 3.3	
.5	49.8 ± 2.1		.2	348.0 ± 7.7	
[KAcetate], with MgCl ₂ (M)			[KAcetate], with MgCl ₂ (M)		
.3	3.0 ± 0.16		.107	16.6 ± 0.06	
.35	5.1 ± 0.25		.15	74.5 ± 2.2	
.4	8.6 ± 0.53	4.9 ± 0.5	.193	146.9 ± 3.5	3.4 ± 0.25
.45	23.0 ± 1.1		.25	276.9 ± 9.5	
.5	33.2 ± 1.3		.275	493.1 ± 27	

Titrations were performed in 10 mM Tris, and salts as noted, pH 7.9.
 * Errors reflect goodness of fit to Equation 1.1
 ** Errors reflect goodness of fit to Equation 1.2

APPENDIX 4

KLENTAQ STRUCTURE DEPENDENCE OF BINDING

63/70mer		
[KCl] (mM)	K_d (nM)	Linkage
50	8.9 ± 0.36	
75	39.3 ± 1.2	
100	99.8 ± 3.6	-3.6 ± 0.07
125	252.4 ± 5.9	
150	500.3 ± 9.1	

63/63mer		
[KCl] (mM)	K_d (nM)	Linkage
50	12.1 ± 0.3	
75	38.5 ± 1.2	
100	89.3 ± 4.4	-3.1 ± 0.11
125	202.3 ± 10.5	
150	387.2 ± 15.7	

63mer		
[KCl] (mM)	K_d (nM)	Linkage
5	33.4 ± 1.3	
10	43.5 ± 1.9	
20	100.3 ± 1.7	-0.98 ± 0.13
35	157.3 ± 7.2	
50	329.7 ± 7.2	

Linkage was determined by fitting data to Equation 1.2. Errors represent goodness of fit to Equation 1.1 for K_d determination and Equation 1.2 for linkage determination.

APPENDIX 5

PH 6 DCIP AND ASCORBIC ACID REACTIONS MEASURED ON-BOARD KC-135.

<i>Control on Plane</i>				<i>Microgravity</i>			
[Asc] mM	τ (msec)	k_{obs} (sec ⁻¹)***	k_1 (M ⁻¹ sec ⁻¹)	[Asc] mM	τ (msec)	k_{obs} (sec ⁻¹)***	k_1 (M ⁻¹ sec ⁻¹)
9.16	305.85	3.27 ± 0.37		9.16	459.36	2.18 ± 0.40	
13.25	94.51	10.58 ± 0.78		13.25	82.60	12.11 ± 0.63	
17.33	94.32	10.60 ± 0.65		17.33	67.51	14.81 ± 0.88	
21.42	62.13	16.10 ± 1.01	850 ± 43*	21.42	66.30	15.08 ± 0.83	852 ± 36*
25.50	56.92	17.57 ± 1.31	1066 ± 75**	25.50	53.03	18.86 ± 1.34	1014 ± 77**
29.58	48.91	20.45 ± 1.77		29.58	43.55	22.96 ± 1.36	
33.67	40.76	24.53 ± 1.93		33.67	31.35	31.90 ± 2.23	
37.75	28.72	34.82 ± 3.02		37.75	29.89	33.45 ± 3.38	
41.83	24.53	40.78 ± 3.90		41.83	29.62	37.78 ± 4.04	
50.00	21.22	47.12 ± 7.75		50.00	N. D.	N. D.	

* k_1 determined by fitting to Equation 2.2, error reflects goodness of fit to this equation.

** k_1 determined by fitting to Equation 2.3, error reflects goodness of fit to this equation.

*** Error reflects goodness of fit of averaged curves to Equation 2.1.

τ and k_{obs} determined by averaging 2-4 shots performed on board KC-135 under appropriate conditions.

APPENDIX 6

PH 9 DCIP AND ASCORBIC ACID REACTIONS MEASURED ON-BOARD KC-135 VS. IN-LAB CONTROL

<i>In-lab Control</i>				<i>Microgravity</i>			
[Asc] mM	τ (msec)	k_{obs} (sec ⁻¹)***	k_1 (M ⁻¹ sec ⁻¹)	[Asc] mM	τ (msec)	k_{obs} (sec ⁻¹)***	k_1 (M ⁻¹ sec ⁻¹)
9.16	504.0	2.1 ± 0.7		9.16	10101.0	0.1 ± 0.05	
13.25	300.4	3.4 ± 0.4		13.25	558.7	1.8 ± 0.06	
17.33	242.9	4.2 ± 0.5		17.33	462.0	2.2 ± 0.1	
21.42	200.5	5.0 ± 0.3	256 ± 3*	21.42	213.1	4.7 ± 0.3	283 ± 23*
25.50	163.7	6.1 ± 0.2	271 ± 6**	25.50	N. D.	N. D.	387 ± 40**
29.58	135.8	7.5 ± 1.3		29.58	146.0	6.9 ± 0.3	
33.67	119.6	8.4 ± .4		33.67	111.3	9.0 ± 0.3	
37.75	100.8	10.0 ± 1.1		37.75	70.95	14.1 ± 0.6	
41.83	91.0	11.1 ± 1.2		41.83	73.1	13.7 ± 1.6	
50.00	77.0	13.0 ± 0.3		50	72.8	13.7 ± 1.3	

* k_1 determined by fitting to Equation 2.2, error reflects goodness of fit to this equation.

** k_1 determined by fitting to Equation 2.3, error reflects goodness of fit to this equation.

*** Errors reflect goodness of fit of averaged curves to Equation 2.1.

Control τ and k_{obs} determined by averaging 10 shots performed in-lab.

Microgravity τ and k_{obs} determined by averaging 2-4 shots on-board the KC-135 aircraft under periods of microgravity.

VITA

Gregory Thompson was born in Baton Rouge, Louisiana, on February 1, 1979. He attended Millsaps College in Jackson, Mississippi, in 1997 where he graduated with a Bachelor of Science in biology in May of 2001. After spending a year at the University of Mississippi Medical Center, Gregory applied to graduate school at Louisiana State University to work with Dr. Vince LiCata on type I DNA polymerases from various organisms. Gregory will pursue a career in the biotechnology industry after graduation.